

Cite this: *Dalton Trans.*, 2024, **53**, 8642

Dibenzoazepine hydrazine is a building block for *N*-alkene hybrid ligands: exploratory syntheses of complexes of Cu, Fe, and Li[†]

Alexander Grasruck,^{‡a} Kristina Schall,^{§a} Frank W. Heinemann,^{Ⓜa} Jens Langer,^{Ⓜb} Alberto Herrera,^a Sybille Frieß,^a Günter Schmid^{Ⓜc} and Romano Dorta^{Ⓜ*a}

The new hydrazine 5*H*-dibenzo[*b,f*]azepin-5-amine (**2**) reacts with P- and Si-electrophiles via deprotonation to afford P(III)-, P(V)-, and TMS-hydrazides **3–8** and with carbonyl electrophiles via acid-free condensation to the *N*-substituted hydrazones **9–12** that are potential *N*-alkene ligands. While β-ketohydrazone **9** and α-dihydrazone **10** react with [Mes(Cu)]₄, [Cu(NCCCCH₃)₄]₂PF₆, and FeCl₂(THF)_{1.5} to afford complexes devoid of alkene interaction, [Cu(OTf)]₂·C₆H₆ reacts with the α-keto hydrazone **11** or with *N,N* dimethylhydrazone **12** to form the neutral dimeric Cu(I) complex **18** with bridging Cu(I)–alkene interactions or the tetrahedral cationic complex **19** in which **12** binds as a bidentate hydrazone–alkene ligand, respectively. The surprising stability of the alkene coordination in complexes **18** and **19** prevents substitutions with, e.g., PPh₃.

Received 12th March 2024,
Accepted 17th April 2024

DOI: 10.1039/d4dt00749b

rsc.li/dalton

Introduction

Hydrazones are a versatile synthetic tool in organic chemistry.¹ In particular, metallated hydrazones are key intermediates in C–C bond forming reactions² and reductions such as the Shapiro reaction.³ However, their application as supporting ligands for metal complexes in synthesis and catalysis is less developed.⁴ For example, hydrazones corresponding to α- and β-diimines (e.g. nacnac type ligands) have different electronic properties through the second hydrazine nitrogen atom.⁵ Some time ago, we and others have introduced 5*H*-dibenzo[*b,f*]azepine as a building block for the synthesis of chiral⁶ and achiral⁷ hemilabile *P*- and *S*-alkene hybrid ligands (Chart 1): Ligands **I** and **II** feature both point and planar chirality, while the superbulky ligand **IV** displays a crystallographic Tolman cone angle of 229°. In order to extend the versatility of this building block we envisaged the corresponding hydrazine

5*H*-dibenzo[*b,f*]azepin-5-amine (**2**) inspired by Grützmacher's 5-amino-5*H*-dibenzo[*a,d*]cycloheptene (tropNH₂).⁸ In this paper, we disclose a multi-gram scale preparation of the new hydrazine **2** and its use for the synthesis of hydrazone-based *N*-alkene hybrid ligands. The coordination chemistry with Li, Fe(II), Cu(II), and Cu(I) is presented. In particular, the Cu(I) species are shown to be additionally stabilized by alkene coordination of the alkene function of the benzoazepine moiety.

Results and discussion

For the realization of new *N*-alkene hybrid ligands, the accessibility of the primary hydrazine **2** on a gram scale had first to be demonstrated: dibenzo[*b,f*]azepine reacts with NaNO₂ under acidic conditions following literature procedures for similar systems⁹ to afford nitrosoamine **1** as yellowish crystals in good yields (Scheme 1). The reduction of **1** with LiAlH₄¹⁰ can be performed on a multi gram scale and yields **2** as a bright yellow crystalline solid. **2** decomposes by N–N bond cleavage under acidic conditions, which must be avoided.

The reaction of **2** with Si- and P-electrophiles is outlined in Scheme 2. Yellow **2** is deprotonated with LDA in THF at RT to afford a red suspension of an orange solid, which is quenched *in situ* with a slight excess of Ph₂PCl or TMSCl to afford **3**¹¹ and **6**, respectively, in very good isolated yields. Similarly, **2** reacts with PBr₂Ph₃¹² in the presence of 1.5 equiv. of NEt₃ to afford the phosphonium bromide **4**. The ¹H NMR spectra for **3** and **4** show characteristic doublets at 4.95 and 11.38 ppm, respectively, for the amine protons due to ²J-coupling to phosphorus. In **6** the NH proton resonates at 3.75 ppm as a broad singlet.

^aDepartment of Chemistry and Pharmacy, Chair of Inorganic and General Chemistry, Friedrich Alexander Universität Erlangen–Nürnberg, Egerlandstraße 1, 91058 Erlangen, Germany. E-mail: romano.dorta@fau.de

^bDepartment of Chemistry and Pharmacy, Chair of Inorganic and General Chemistry and Chair of Inorganic and Organometallic Chemistry, Friedrich Alexander Universität Erlangen–Nürnberg, Egerlandstraße 1, 91058 Erlangen, Germany

^cSiemens Energy Global GmbH & Co. KG, New Energy Business – Technology & Products, Freyeslebenstraße 1, 91058 Erlangen, Germany

[†]Electronic supplementary information (ESI) available: X-ray crystallographic information, NMR spectra. CCDC 2338469–2338477. For ESI and crystallographic data in CIF or other electronic format see DOI: <https://doi.org/10.1039/d4dt00749b>

[‡]Current address: IBU-tec advanced materials AG, Hainweg 9-11, 99425 Weimar, Germany.

[§]Present address: 3M Dach, 40721 Hilden, Germany.



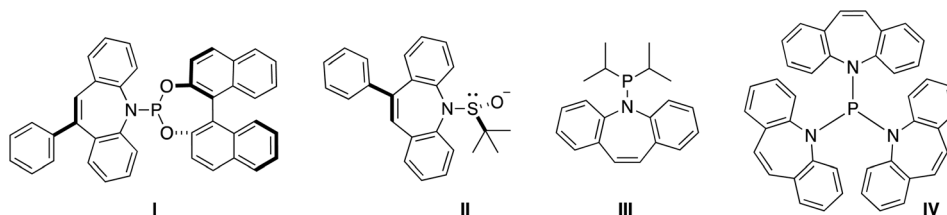
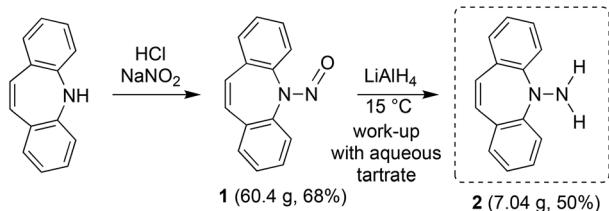
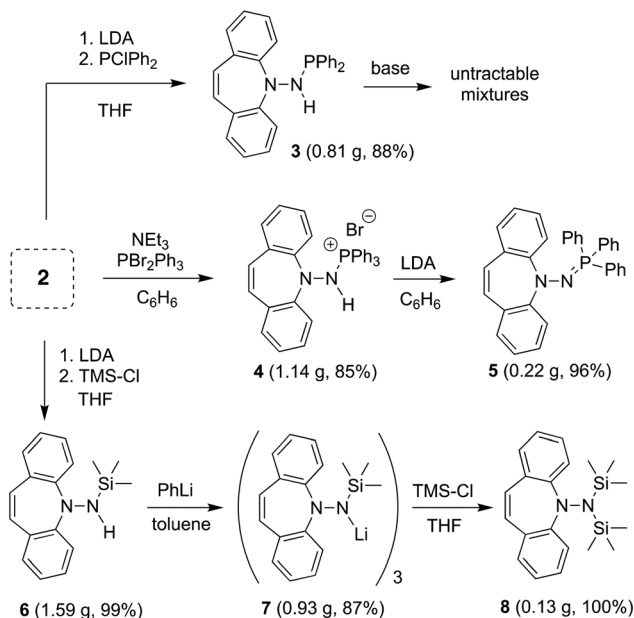


Chart 1

Scheme 1 Synthesis of the new dibenzo[*b,f*]azepine derived hydrazine 2.

Scheme 2 Reactions of 2 with P(III), P(V), and the TMS-Cl electrophiles.

The ^{31}P NMR spectra of 3 and 4 show a singlet resonance at 49.1 and 38.9 ppm, respectively (2J -couplings are not resolved).

While the deprotonation of 3 to the corresponding amidophosphine does not afford clean, isolable products with a variety of bases, such as PhLi,¹³ from 4, the second equivalent of HBr is eliminated with LDA liberating the iminophosphine 5 as a yellow powder in practically quantitative yields. Contrary to *N*-alkyliminophosphines,¹⁴ 5 is air-stable and resistant to hydrolysis. 5 was needed in this project as potential imidation reagent¹⁵ for carbonyl compounds (*vide infra*). 6 is smoothly deprotonated by PhLi in toluene to form the trimeric lithium complex 7 as an orange powder in good yield,¹⁶ whose ^1H

NMR reveals broad signals due to fluxional behavior. Attempts to prepare the analogous potassium salt by reacting 6 with benzyl potassium or KH afforded untractable products. Reacting 7 with an additional equivalent of TMSCl quantitatively yields pure 8 that does not need further purification.¹⁷ ^1H NMR shows one singlet at 0.25 ppm for the TMS groups and a characteristic singlet at 5.99 ppm for the alkene protons of the azepine. As with 5, 8 is a potential hydrazide transfer reagent (*vide infra*).¹⁸

Single crystal X-ray diffraction analysis of 7 revealed a C_3 -symmetric trimeric structure containing three lithium atoms forming an equilateral triangle (Fig. 1). The average Li–N bond length of 1.988 Å is in the range of reported values^{19,16b} and similar to the corresponding bond in complex 13 (*vide infra*). The lithium-bridging hydrazido *N*-donors are tetrahedral, while the azepine ring *N*-atoms N1, N3 and N5 are trigonal planar (sum of bond angles $\sum \angle(\text{N}) \approx 360^\circ$). One of the two

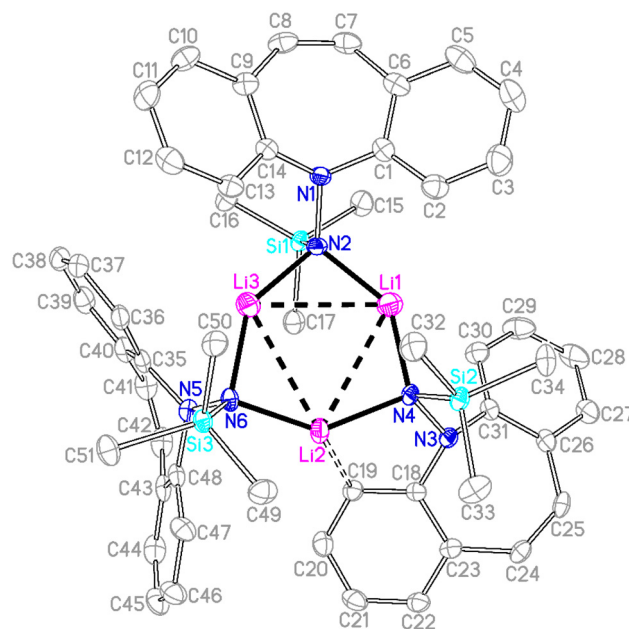
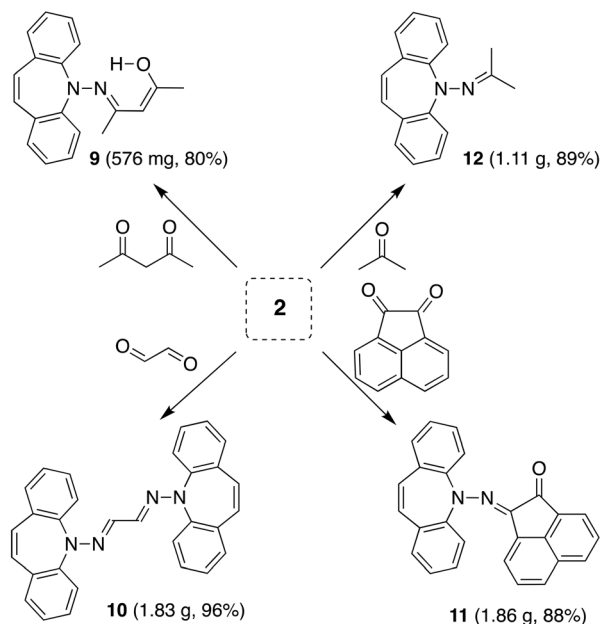


Fig. 1 Crystal structure of one of two independent molecules of 7 (50% probability ORTEP, H atoms are omitted). Selected bond lengths (Å) and angles (deg): Li1–N2 1.933(7), Li3–N2 1.989(7), Li1–Li3 2.960(9), N1–N2 1.479(4), Si1–N2 1.736(3), Si1–C16 1.866(4), Li2–C19 2.429(7) Å; C1–N1–C14 114.8(3), C1–N1–N2 117.2(3), Li1–N2–Li3 98.0(3), N2–Li1–N4 139.8(4), N6–Li2–N4 138.1(3).





Scheme 3 Condensation of **2** with carbonyl compounds to hydrazones.

independent molecules in the asymmetric unit exhibits an agostic interaction ($\text{Li2}\cdots\text{C19}$) at a distance of 2.431 Å.²⁰ Similar Agostic interactions in this position of the dibenzo[*b,f*]azepine backbone have also been observed for Ru(II) complexes with P-alkene ligands.²¹

The reaction of **2** with carbonyl electrophiles is summarized in Scheme 3. With acetylacetone the mono substituted β -keto-hydrazone **9** is isolated in high yield after stirring for 10 d in EtOH at room temperature and crystallization. Long reaction times are necessary because the usual catalysts cannot be used due to the instability of **2** towards Brønsted acids.²² The ¹H NMR spectrum shows characteristic resonances for the OH

and alkene protons at 13.1 and 6.75 ppm, respectively. Condensation of a second equivalent of **2** was attempted in three ways: (i) *in situ* alkylation of **9** with $[\text{OMe}_3][\text{BF}_4]$ followed by addition of **2** under basic conditions,²³ (ii) reaction of **9** with bis-silyl hydrazide **8** at 60 °C (with the intention to drive the reaction by forming $(\text{TMS})_2\text{O}$), and (iii) by an acid-free aza-Wittig reaction² employing imino-phosphine **5** (Scheme 2). While the first two methods gave no reaction, a mixture of acetylacetone with **5** led to decomposition at 90 °C (at lower T no reaction takes place), even though $\text{P}(\text{O})\text{Ph}_3$ was identified in the crude product mixture. With hexafluoroacetylacetone, on the other hand, **5** reacts as a base in THF at 50 °C to afford the iminium salt $[\text{5-H}][\text{F}_3\text{C}(\text{O})\text{CCC}(\text{O})\text{CF}_3]$ (an analogue of **4**).²⁴ Condensation of **2** with glyoxal quantitatively affords **10**, which turned out to be hydrolysis resistant and which precipitates as a mixture of isomers as evinced by its ¹H NMR spectrum. Such yellow CDCl_3 NMR solutions of **10** turn orange within hours and show the expected peak pattern of one sole symmetrical isomer.²⁵ XRD analysis revealed the exact configuration of **10** in the crystal and shows the *trans*-isomer with a perfectly planar tetraazahexadiene chain (Fig. 3). The terminal azepine N-atoms are very slightly pyramidalized ($\sum\angle(\text{N}) = 356^\circ$), and the C15–N2 bond length of 1.290 Å is in the expected range.²⁶ With acenaphthenequinone, **2** reacts only in a one-to-one ratio to the α -keto-hydrazone **11**,²⁷ albeit in excellent yields. The ¹H NMR spectrum shows a characteristic singlet at 6.9 ppm suggesting C_s symmetry in solution. In the crystal, the symmetry is lower with the dibenzoazepine moiety tending into coplanarity with the acenaphthenequinone substituent contrasting aniline-based BIANs (Fig. 2, right).²⁸ The nitrogen atoms lie in the quinone plane within *ca.* 5°, while the dibenzo[*b,f*]azepine moiety is twisted out of plane by 23° (average torsion angle along C5–C1–C19–C20 in four independent molecules). The N1–N2 bond distance of 1.37 Å indicates double bond character. Finally, hydrazone **12** forms upon condensation of **2** with acetone. The ¹H NMR spectrum shows two

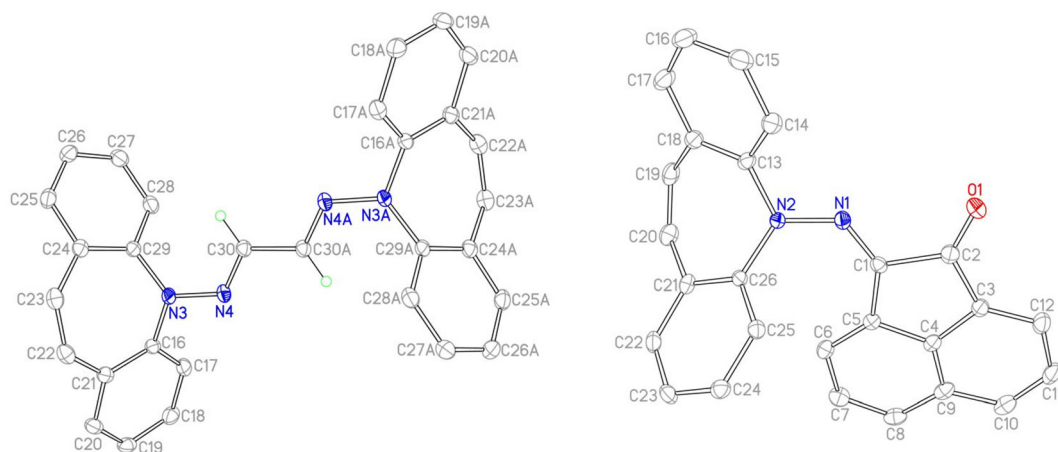
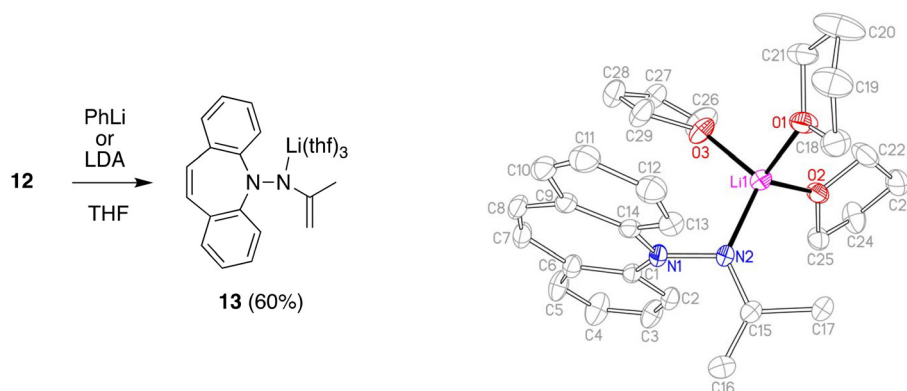


Fig. 2 Crystal structures of **10** (left, one of two independent molecules) and **11** (right, one of four independent molecules). ORTEPs are drawn at 50% probability, H atoms are omitted. Selected bond lengths (Å) and angles (deg) for **10**: C15–C15A 1.444(2), N1–N2 1.3741(12), N2–C15 1.2904(13), N1–C1 1.4278(13), C7–C8 1.3426(17), N2–N1–C1 113.37(8), N2–N1–C14 123.22(8), C15–N2–N1 119.95(9); for **11**: C2–O1 1.214(3), N1–N2 1.354(2), C1–N1 1.296(3), N2–C13 1.437(3), C1–C2 1.517(3), C19–C20 1.340(3), N2–N1–C1 124.17(17), N1–C1–C2 114.39(17).





Scheme 4 Synthesis and crystal structure of **13** (50% probability ORTEP, H atoms are omitted). Selected bond lengths (Å) and angles (deg): Li1–N2 1.956(4), N2–C15 1.370(2), C15–C16 1.346(3), C15–C17 1.514(3), N1–N2 1.443(2), N1–C1 1.413(2), C7–C8 1.327(3); N1–N2–Li1 114.44(14), C15–N2–Li1 132.58(16), C16–C15–C17 119.77(18).

singlets at 1.98 and 2.28 ppm for the methyl groups and a singlet at 7.09 ppm for the alkene protons.

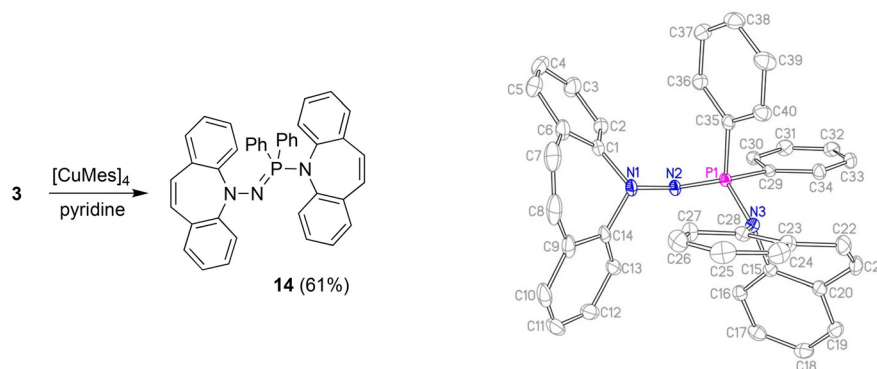
Deprotonation of **12** with lithium di-isopropylamide (LDA) or PhLi in THF solution affords the deep red aza-enolate **13** (eqn (1)). The enamine protons resonate as singlets at 2.75 and 2.96 ppm in the ^1H NMR spectrum. There is no indication for conjugation between the π -systems of the enamide and the dibenzo[*b,f*]azepine. The crystal structure of **13** has approximate C_s symmetry consistent with its solution structure (Scheme 4). Solvation by three THF molecules creates together with the hydrazido N-donor a tetrahedral coordination geometry around lithium and prevents higher aggregation (*cf.* complex **7** above). The N atoms are trigonal planar with $\sum\angle(\text{N1}) = 358.5^\circ$ and $\sum\angle(\text{N2}) = 360.0^\circ$, and the N–Li distance of 1.956 Å parallels the values observed in **7**.²⁹ The delocalized nature of the enamide function is reflected in its planar geometry and the short N2–C15 bond distance of 1.370 Å indicating double bond character.³⁰ The enamide moiety is oriented perpendicular to the unusually planar dibenzo[*b,f*]azepine backbone with the C15–C16 double bond (1.346 Å) pointing towards it. Normally, the azepine ring displays a boat configuration due to its antiaromatic character,³¹ which has been used to great effect to install stable planar chirality in similar *P*- and *S*-alkene ligand systems.³² In addition, the C7–C8 bond (1.327 Å) clearly has double bond character and is not in conjugation with the benzene rings. Conjugative effects between the π -systems are also excluded because the N1–N2 distance (1.443 Å) identifies it as a single bond and because of the aforementioned perpendicular orientation of the *N*-substituents. The planarity of the system is therefore explained in terms of steric, rather than electronic, preference. Nevertheless, this is a rare example, in which the planar structure is stable enough to be caught in the crystal.

With the well characterized potential ligands **3**, **5**, **7**–**13** at hand, their coordination chemistry with iron and copper was explored, because, ultimately, we are interested in the stabilization of reactive hydrides of first-row transition metal-hydrides for the reduction of CO_2 .³³ The synthesis of Cu(I) amido complexes was attempted with ligands **3**, **6**–**8** (Scheme 2). **3** reacts

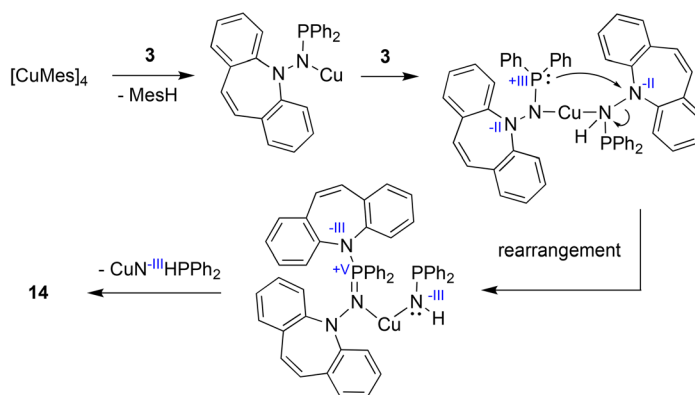
with $[\text{Cu}(\text{Mes})_4]$ in pyridine or THF solution and a beige solid is isolated (Scheme 5). Against expectations, crystallographic analysis revealed the metal-free imino-phosphine **14**, in which the tetrahedral phosphorus atom is bound to two phenyl groups, one dibenzo[*b,f*]azepine, and one hydrazine dibenzo[*b,f*]azepine moiety. The P1–N2 bond distance of 1.598 Å corresponds to a double bond,³⁴ whereas the P1–N3 single bond measures 1.692 Å.³⁵ The ^{31}P nucleus resonates as a singlet at 16.9 ppm. The mechanism outlined in Scheme 6 rationalizes the outcome of the reaction of $[\text{Cu}(\text{Mes})_4]$ with two equivalents of **3**. NMR control experiments of the reaction revealed rapid formation of mesitylene on deprotonation of **3** by $[\text{Cu}(\text{Mes})_4]$ in the proton spectrum and a broad ^{31}P resonance at 58 ppm of a major side product, which we attribute to CuNHPPH_2 . We assume that the initially formed unsaturated copper amido complex is stabilized by coordination of a second equivalent of neutral ligand, triggering the intramolecular redox rearrangement to **14** upon elimination of CuNHPPH_2 . The N–N cleavage reduces two nitrogen atoms from -II to -III, while the P(III) is oxidized to P(V), so overall this reaction could be termed an oxidative addition of an N–N bond to P(III). Oxidation of phosphorous by Cu(I) is excluded because no precipitation of metallic Cu was observed.

In contrast to phosphine hydrazide **3**, the silyl hydrazide **6** does not react with the Cu(I) precursors $[\text{MesCu}]_4$ (Mes = mesityl anion) and $[\text{Cu}(\text{O}^t\text{Bu})_4]$ to the Cu(I) silyl amido complex,³⁶ presumably because the copper precursors are not basic enough. Also **7** and **8** were tried in reactions with CuCl in a bid to obtain the copper amide *via* salt metathesis or under the elimination of TMSCl, respectively.³⁷ The reactions with **7** in varying metal to ligand ratios (cuprates were also envisioned) resulted in untractable mixtures,³⁸ while **8** did not react with CuCl even at 70 °C. The reaction of **9** with $[\text{Cu}(\text{Mes})_4]$ results in dark brown reaction mixtures that show no ^1H NMR signals, indicative of a disproportionation reaction to metallic copper and a Cu(II) complex **15** (eqn (1)),³⁹ which was confirmed by single crystal X-ray diffraction analysis (Fig. 3).⁴⁰ The roughly square planar complex (dihedral angle between coordination planes: 9.7° (ref. 41)) is supported by two molecules of deprotonated N,O-coordinated **9** and





Scheme 5 Synthesis and crystal structure of **14** (50% probability ORTEP, H atoms are omitted). Selected bond lengths (Å) and angles (deg): P1–N2 1.5977(12), P1–N3 1.6919(12), N1–N2 1.4611(16), N1–C1 1.4381(19), N3–C15 1.4453(18), N1–N2–P1 111.31(9), N2–P1–N3 122.47(6), N3–P1–C29 103.55(6), N3–P1–C35 104.05(6), C29–P1–C35 105.14(7), C15–N3–P1 118.54(9), C1–N1–N2–P1 117.32(11).



Scheme 6 Proposed mechanism for the formation of **14**.

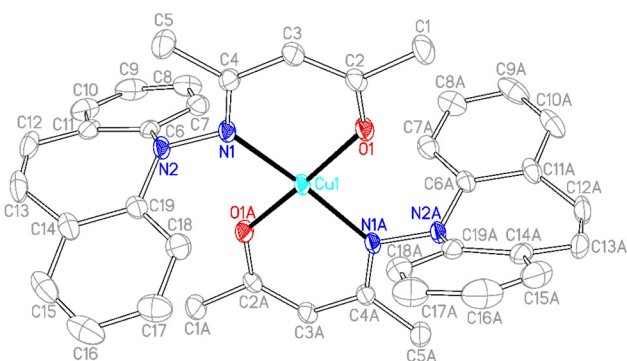
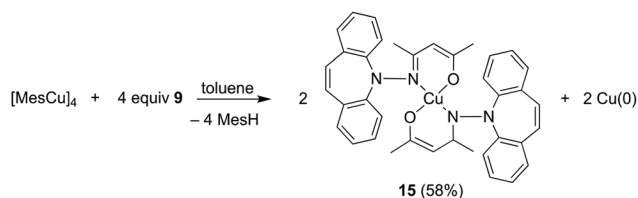


Fig. 3 Crystal structure of **15** (50% probability ORTEP, H atoms are omitted). Selected bond lengths (Å) and angles (deg): Cu1–O1 1.8903(14), N1–N2 1.432(2), Cu1–N1, 2.0041(16), O1–C2 1.277(3), N1–C4 1.323(3), C2–C3 1.376(3), C3–C4 1.418(3), O1–Cu1–O1A 173.98(13), N1–Cu1–N1A 172.26(12), O1–Cu1–N1 90.80(6), O1–Cu1–N1A 89.60(6), C4–N1–N2 112.89(17), C2–C3–C4 125.5(2).

has crystallographic centrosymmetry. The *trans* positioned O and N donors span angles of 172–174° and their distances to the metal center are in the range of reported values.⁴² The Cu–N bond is slightly longer due to the steric pressure exerted by the

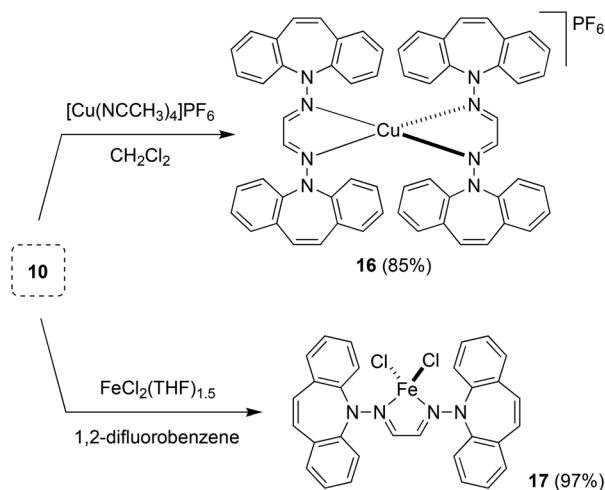
dibenzo[*b,f*]azepine residue, which is oriented perpendicularly to the Cu–nac plane.



(1)

Two equivalents of **10** react with $[\text{Cu}(\text{NCCH}_3)_4]\text{PF}_6$ to yield complex **16** as an orange powder (Scheme 7).⁴³ Long reaction times (*ca.* 3 d) are required to ensure the coordination of the second ligand equivalent. NMR spectra do not indicate ligand alkene coordination and support a complex of high symmetry in solution. **10** also reacts with $\text{FeCl}_2(\text{THF})_{1.5}$ to afford red-brown crystals of **17** in excellent yield.⁴⁴ The crystal structure suffered from substantial disorder, caused by the presence of different conformers. The major conformer, which occupied 78% of the lattice sites, showed a transoid



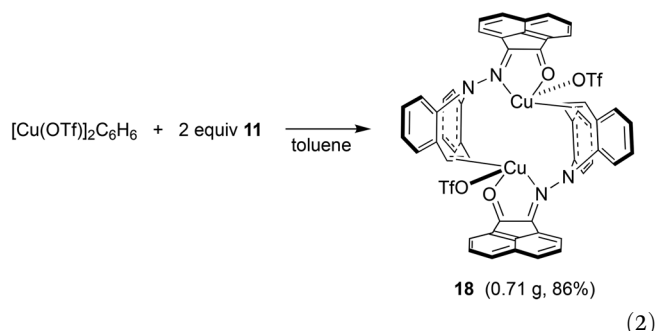


Scheme 7 Synthesis of the tetrahedral Cu(I) and Fe(II) complexes **16** and **17**.

arrangement of the dibenzoazepine moieties, and a distorted tetrahedral coordination geometry around iron (Fig. 4). The conformers are defined by the relative orientations of the dibenzo[*b,f*]azepine moieties to each other and suggest low energy barriers between them.⁴⁵ The nitrogen, iron, and imine carbon atoms are coplanar, and azepine N atoms are pyramidalized ($\sum \angle(\text{N}2) = 345.41^\circ$, $\sum \angle(\text{N}4) = 343.05^\circ$). The C1–N1 and C1–C1 distances do not significantly change compared to the free ligand, indicating redox-neutral coordination.

In contrast to the synthesis of complex **15**, disproportionation reactivity is suppressed by the use of the α -keto-hydrazone **11**. It reacts with $[\text{Cu}(\text{OTf})_2]\cdot\text{C}_6\text{H}_6$ to form the dinuclear complex **18** within minutes (eqn (2), Cu(I) halides are unreactive).⁴⁶ The ^1H NMR spectrum shows 16 individual proton

resonances indicating a low-symmetry, rigid structure. The diastereotopic dibenzoazepine alkene protons resonate as doublets at 6.27 and 4.74 ppm. Indeed, the crystal structure reveals a C_2 -symmetric dinuclear complex with pseudo-tetrahedral copper centers reminiscent of triene–Cu(I)–triflates (Fig. 5).⁴⁷ Each α -keto-hydrazone coordinates one copper atom in a bidentate manner, while the alkene function bridges onto the neighboring copper atom. The coordinated C=C double bonds are elongated from 1.341 Å in the free ligand to 1.381 Å, which is on the long side of comparable values.⁴⁸ The copper atoms are separated by 4.58 Å, and the naphthalene moieties are π -stacked at roughly 3.5 Å (C4...C30) and offset.⁴⁹ Due to the fact that the ligands bridge the metals, there is no need for pyramidalization of the dibenzoazepine N atoms ($\sum \angle(\text{N}2) = 355^\circ$, $\sum \angle(\text{N}4) = 353^\circ$), contrasting their usual sp^3 -hybridization encountered in bidentate coordination modes in mononuclear complexes of such hybrid ligands (*cf.* **19** below). The remaining coordination sites are occupied by the triflate anion with a Cu–O contact of 2.232 Å,⁵⁰ thereby securing an 18 valence electron count.⁵¹



Hydrazone **12** cleanly reacts⁵² with $[\text{Cu}(\text{OTf})_2]\cdot\text{C}_6\text{H}_6$ in CH_2Cl_2 solution to complex **19**, which is isolated as gold-yellow powder in excellent yields (eqn (3)). The NMR spectra reflect a highly symmetric complex, and the low frequency shift of the singlet resonance of the alkene protons at 6.54 ppm by 0.5 ppm compared to the free ligand indicates alkene coordination. In fact, X-ray analysis authenticated the bidentate coordination of the ligands through the imine nitrogen and the azepine C=C double bond (Fig. 6). The copper atom has tetrahedral coordination geometry with an outer-sphere OTf^- counterion. While the Cu–N distances are in the expected range for this type of structures,⁵³ the Cu–C bonds are slightly longer than in most reported structures at 2.194–2.288 Å.⁵⁴ The dibenzo[*b,f*]azepine nitrogen atoms are pyramidalized ($\sum \angle(\text{N}1) = 333^\circ$ and $\sum \angle(\text{N}2) = 335^\circ$) due to the bidentate coordination mode of the ligand, which is also a recurring observation in complexes of bidentate dibenzoazepine-based chiral *P*- and *S*-alkene ligands.⁵⁵ The average C–C double bond is similar to the values found in complex **18** and is slightly elongated to 1.368 Å compared with the uncoordinated alkene in the aza-enolate **13** (1.327 Å). This is consistent with Cu(I) alkene coordination involving mostly σ -donation and very little π -back donation.⁵⁶ However, the coordinated alkene functions in complexes **18** and **19** resist substitution by PPh_3 , CO, CO_2 , phenyl isocyanate, or dicyclohexylcarbodiimide.

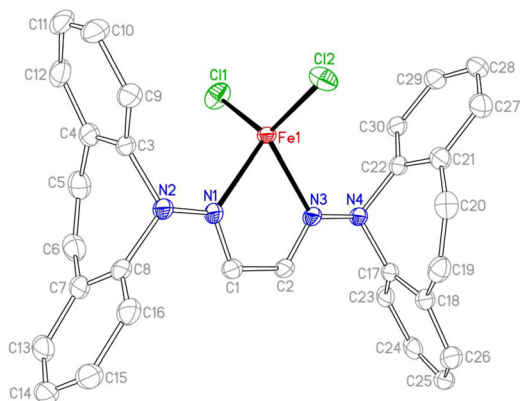


Fig. 4 Crystal structure of one of three conformers of **17** (50% probability ORTEP, H atoms and solvent molecules are omitted). Selected bond lengths (Å) and angles (deg): Fe1–Cl1 2.220(2), Fe1–N1 2.137(2), N1–C1 1.292(3), C1–C2 1.458(3), Cl1–Fe1–Cl2 126.68(6), N1–Fe1–N3 77.14(7), N1–N2–C3 113.22(16), N1–N2–C8 117.00(17), C3–N2–C8 115.19(16), C1–N1–N2 120.75(18), N2–N1–Fe1 125.85(13), C1–N1–Fe1 113.33(14).



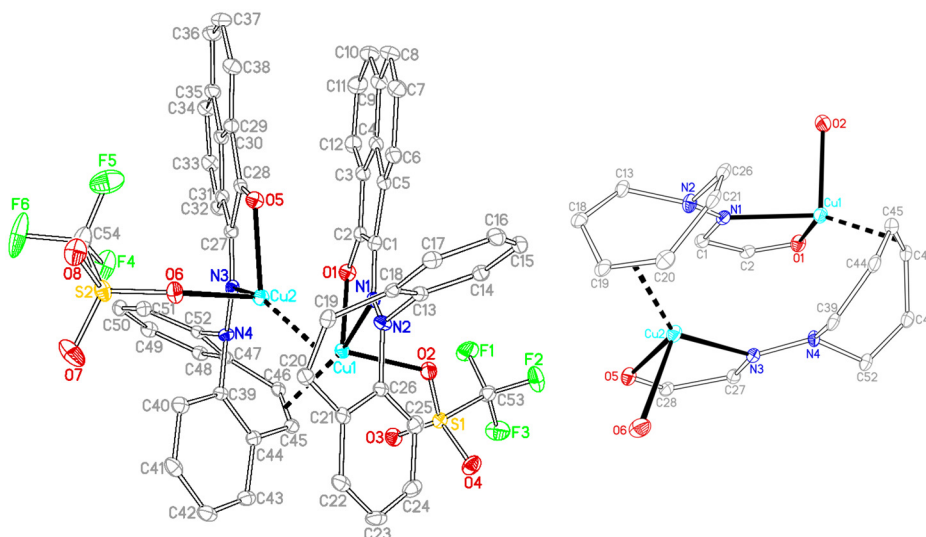
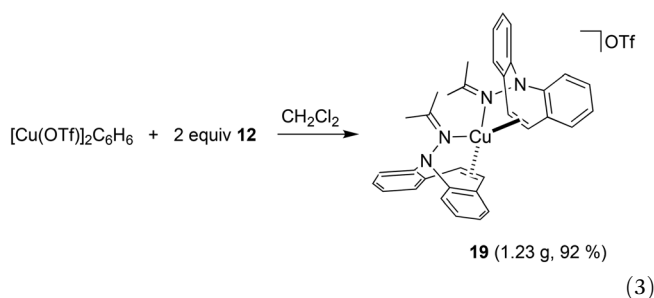


Fig. 5 Crystal structure of **18** with its core structure to the right (50% probability ORTEP, H atoms and solvent molecules are omitted). Selected bond lengths (Å) and angles (deg): Cu1–O1 2.0590(13), Cu1–O2 2.2263(13), Cu1–N1 2.1358(15), Cu1–C45 2.1026(18), Cu1–C46 2.0518(18), C45–C46 1.381(3), Cu2–O5 2.0537(13), Cu2–O6 2.2391(13), Cu2–N3 2.1121(15), Cu2–C19 2.0559(18), Cu2–C20 2.0872(18), C19–C20 1.381(2), N1–N2 1.344(2), N3–N4 1.344(2), O1–Cu1–N1 80.23(5).



Conclusion

The new hydrazine **2** is accessible in multi-gram scales and is a useful building block for the synthesis of *N*- and *P*-alkene hybrid ligands and iminophosphines **5** and **14**, the latter being accessible by a Cu(I) mediated reaction. The neutral and anionic hydrazone derived *N*-alkene ligands are readily prepared on gram-scales and show a versatile coordination behaviour. While **8** was not suitable for Cu(I) complexes, a bicoordinated Cu(II) complex was isolated. α -keto hydrazone **11** and the *N,N*-dimethyl hydrazone **12** form the alkene coordinated Cu(I) complexes **18** and **19**, which sport unexpectedly strong alkene interactions that resist PPh₃ and CO substitution. Moreover, we think that the tricyclic hydrazine **2** is of interest to pharmaceutical/medicinal chemistry and developments along these lines are currently being pursued in our laboratories.

Experimental details

All reactions were carried out under anaerobic and anhydrous conditions, using standard Schlenk and glovebox techniques unless otherwise stated. Et₂O, THF, benzene, *n*-hexane and *n*-pentane were distilled from purple Na/benzophenone solutions, toluene from Na, C₆D₆ from Na/K alloy, CH₂Cl₂ and 1,2-difluorobenzene from CaH₂, and NEt₃ from K. CDCl₃ and CD₂Cl₂ were degassed with three freeze–pump–thaw cycles and then kept over activated molecular sieves (4 Å) in the glovebox. LiAlH₄ was purified by filtration of a concentrated Et₂O solution over glass fiber filter (Whatman GF/B) and subsequent evaporation to a snow-white solid. [CuMes]₄,⁵⁷ [Cu(NCCH₃)₄]PF₆,⁵⁸ and [Cu(OTf)]₂·C₆H₆,⁵⁹ were prepared according to published procedures. Technical solvents were pre-purified by distillation on a rotary evaporator. NMR spectra were recorded on

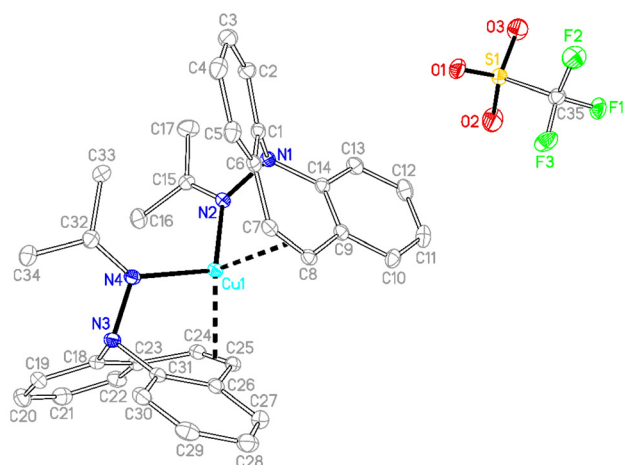


Fig. 6 Crystal structure of **19** (50% probability ORTEP, H atoms are omitted). Selected bond lengths (Å) and angles (deg): Cu1–N2 2.0460(18), Cu1–N4 2.0823(19), Cu1–C7 2.223(2), C7–C8 1.370(3), C24–C25 1.366(3), Cu1–C8 2.280(2), Cu1–C24 2.268(2), Cu1–C25 2.194(2), N1–N2 1.470(3), N3–N4 1.471(3), N4–C32 1.286(3), N2–C15 1.285(3), N2–Cu1–N4 113.89(7), N2–Cu1–C7 92.26(8), N4–Cu1–C24 90.33(8), C32–N4–Cu1 135.03(16), C15–N2–Cu1 127.37(16).



a JOEL EX 400 (400.5 MHz), JOEL EX 270 (270 MHz), Bruker Avance DPX300 NB (300 MHz) and Bruker Avance III HD (600 MHz). Chemical shifts δ are indicated in ppm and ^1H - and ^{13}C NMR shifts refer to the solvent signal as an internal standard (CDCl_3 , $\delta = 7.25$; C_6D_6 , $\delta = 7.16$).⁶⁰ Signal multiplicities are given as s (singlet), d (doublet), t (triplet), q (quartet), oct (octet) or m (multiplet). The raw data were processed with Mestrec. The elemental analyses (EAs) of new products were determined with a Euro EA 3000 (Euro Vector).

5-Nitroso-5*H*-dibenzo[*b,f*]azepine (1)

Dibenzo[*b,f*]azepine (77.7 g, 402 mmol) was suspended in EtOH (800 ml) and cooled to 0 °C before conc. HCl (280 ml) was added. After 15 min a solution of NaNO_2 (30.5 g, 442 mmol) in H_2O (250 ml) was added dropwise *via* addition funnel over 40 min. The reaction mixture turned brown before a brown precipitate formed. The suspension was stirred for 1 h at 0 °C and filtered with a frit. The solid was slurried in EtOH (300 ml), filtered and washed with petrol ether (200 ml). The crude was extracted with DCM (400 ml) and filtered over activated charcoal to remove remaining inorganic salts. The brownish solution was concentrated to 150 ml and *n*-pentane was added to promote crystallization. After cooling overnight at -30 °C, the mother liquor was removed, and the yellowish crystals were dried in HV. The product was recrystallized from boiling toluene (400 ml) to obtain slightly yellowish crystals. The solvent was decanted, and the crystals were washed with *n*-pentane (2 × 50 ml) before drying in HV (60.4 g, 68%). ^1H NMR: (600 MHz, CDCl_3) δ (ppm) = 7.62 (d, 1H, ArH, $^3J_{\text{H,H}} = 6$ Hz), 7.56–7.53 (m, 1H, ArH), 7.49–7.38 (m, 5H, ArH), 7.15 (d, 1H, ArH, $^3J_{\text{H,H}} = 6$ Hz), 6.89; 6.84 (dd, 2H, ArH, $^4J_{\text{H,H}} = 12$ Hz, $^3J_{\text{H,H}} = 30$ Hz). ^{13}C NMR (101 MHz, CDCl_3) δ (ppm) = 140.83 (s), 136.25 (s), 132.81 (s), 132.16 (s), 130.49 (s), 130.43 (s), 130.17 (s), 129.85 (s), 129.61 (s), 129.23 (s), 129.16 (s), 128.94 (s), 127.61 (s), 126.09 (s). EA found: C 75.39%, H 4.46%, N 12.47%; calculated for $\text{C}_{14}\text{H}_{10}\text{N}_2\text{O}$: C 75.66%, H 4.54%, N 12.60%.

5*H*-Dibenzo[*b,f*]azepin-5-amine (2)

1 (15.4 g, 68.4 mmol) was dissolved in dry THF (250 ml) and cooled to 15 °C. A solution of LiAlH_4 (2.72 g, 71.8 mmol) in THF (30 ml) was added dropwise, so that the gas formed at a controlled rate. The resulting dark greenish solution was stirred for 1 h at 15 °C. The cooling bath was removed, and stirring was continued for 15 h at RT. The reaction mixture was quenched with aqueous sodium tartrate solution (20 g of $\text{C}_4\text{H}_4\text{Na}_2\text{O}_6 \cdot 2\text{H}_2\text{O}$ in 180 ml of H_2O) and Et_2O (300 ml) was added. The phases were separated, and the aqueous phase was extracted with Et_2O (3 × 200 ml). The combined organic phases were dried over MgSO_4 , and the solvent was removed. The product was purified by column chromatography with deactivated silica (Hex/EtOAc/ NEt_3 , 8:1:1) and obtained as a yellow crystalline solid (7.04 g, 50%). ^1H NMR: (600.13 MHz, CDCl_3) δ 7.33–7.23 (m, 4H, ArH), 7.09–7.01 (m, 4H, ArH), 6.77 (s, 2H, ArH), 4.29 (s (br), 2H, NH_2). ^{13}C NMR: (150.9 MHz, CDCl_3) δ 152.7 (s), 132.4 (s), 130.9 (s), 129.2 (s), 129.1 (s), 123.7

(s). EA found: C 81.15%, H 5.81%, N 13.07%; calculated for $\text{C}_{14}\text{H}_{12}\text{N}_2$: C 80.74%, H 5.81%, N 13.45%.

N-(Diphenylphosphanyl)-5*H*-dibenzo[*b,f*]azepin-5-amine (3)

A solution of LDA (249 mg, 2.33 mmol) in THF (3 ml) was added dropwise to a solution of 2 (530 mg, 2.33 mmol) in THF (5 ml). While stirring for 1 h, the reaction mixture turned red and an orange precipitate formed. The reaction mixture was cooled to -30 °C and was added dropwise to a solution of PPh_2Cl (525 mg, 2.38 mmol) in THF (5 ml), which was cooled to -30 °C. The formed yellow solution was stirred for additional 2 h. The solvent was removed, the residue was extracted with benzene (15 ml) and filtered over cotton and Celite in a pipette. The yellow solution was cooled to -30 °C and subsequently the frozen benzene was sublimed in HV. Afterwards the product was slurried in *n*-pentane (15 ml) for 1 h, cooled to -30 °C and filtered cold. The precipitate was washed with *n*-pentane (6 ml), filtered again and dried in HV to afford a yellow powder (811 mg, 88%). ^1H NMR: (400 MHz, C_6D_6) δ 7.45–7.41 (m, 4H, ArH), 6.93–6.87 (m, 8H, ArH), 6.73–6.65 (m, 6H, ArH), 6.33 (s, 2H, ArH), 4.95 (d, 1H, NH, $^2J_{\text{H,P}} = 32$ Hz) ^{13}C NMR: (101 MHz, C_6D_6) δ 152.8 (s), 139.6 (s), 139.5 (s), 132.8 (s), 132.6 (s), 132.3 (s), 131.0 (s), 128.74 (s), 128.4 (s), 128.5 (s), 127.7 (s), 123.4 (s), 119.2 (s). ^{31}P NMR: (162 MHz, C_6D_6) δ 49.1 (s). EA found: C 79.88%, H 5.38%, N 6.84%; calculated for $\text{C}_{26}\text{H}_{21}\text{N}_2\text{P}$: C 79.58%, H 5.39%, N 7.14%.

Dibromotriphenyl- λ^5 -phosphine (PBr_2Ph_3)⁶¹

Triphenylphosphine (3.00 g, 11.4 mmol) was suspended in acetonitrile (15 ml) and the mixture was cooled down to 0 °C. Bromine (1.82 g; 11.4 mmol; 0.58 ml) was added dropwise *via* syringe and stirring was continued for 1 h. To remove the excess of bromine, a solution of triphenyl phosphine (0.60 g diluted in 10 ml acetonitrile) was added. The white precipitate was separated by filtration, washed with acetonitrile (15 ml) and dried under reduced pressure to yield an off-white powder (4.67 g, 97%). ^1H NMR (600 MHz, $\text{DMSO}-d_6$) δ 7.64–7.57 (m, 9H, ArH), 7.57–7.51 (m, 6H, ArH). ^{31}P NMR: (243 MHz; $\text{DMSO}-d_6$) δ 25.5 (s).

((5*H*-Dibenzo[*b,f*]azepin-5-yl)amino)triphenyl-phosphonium bromide (4)⁶²

PBr_2Ph_3 (1.03 g, 2.43 mmol) was dissolved in benzene (7 ml) and a solution of 2 (505 mg, 2.43 mmol) and NEt_3 (369 mg, 3.65 mmol) in benzene (7 ml) was added slowly. The yellow reaction mixture was stirred for 20 hours, then the solvent was removed by sublimation. The air stable light-yellow solid was washed with water (50 ml), Et_2O (40 ml) and dried under reduced pressure to obtain an off-white powder (1.14 g, 85%) ^1H NMR (400 MHz, CDCl_3) δ 11.38 (d, $J = 41.6$ Hz, 1H, NH), 8.47 (d, $J = 8.2$ Hz, 2H), 7.69 (ddd, $J = 13.1, 8.2, 1.4$ Hz, 6H), 7.61 (td, $J = 7.5, 1.6$ Hz, 3H), 7.42 (td, $J = 7.8, 3.5$ Hz, 6H), 7.31 (ddd, $J = 8.4, 7.3, 1.7$ Hz, 2H), 6.93 (td, $J = 7.5, 1.0$ Hz, 2H), 6.84 (dd, $J = 7.6, 1.6$ Hz, 2H), 6.46 (s, 2H). ^{31}P NMR (162 MHz, CDCl_3) δ 39.06 (d, $J = 38.0$ Hz). ^{13}C NMR (101 MHz, CDCl_3) δ 149.54 (d, $J = 2.5$ Hz), 134.77 (d, $J = 2.9$ Hz), 134.33 (s), 134.2



(s), 131.9 (s), 130.2 (s), 130.0 (s), 129.4 (s), 129.2 (s), 128.1 (s), 124.7 (s), 122.5 (s), 120.2 (s), 119.14 (s). EA found: C 70.05%, H 4.67%, N 5.02%; calculated for C₃₂H₂₆N₂PBr: C 69.95%, H 4.77%, N 5.10%.

N-(5*H*-Dibenzo[*b,f*]azepin-5-yl)-1,1,1-triphenyl-λ⁵-phosphanimine (5)

4 (263 mg, 0.476 mmol) and LDA (51.0 mg, 0.476 mmol) were placed in a vial and suspended in benzene (10 ml). The initial colorless suspension turned immediately yellow and stirring was continued for 2.5 h. Afterwards the reaction mixture was centrifuged at 6000 rpm for 6 minutes to separate the LiBr from the mother liquor. The benzene was removed by sublimation and the remaining solid was dried under reduced pressure. The product is obtained as a yellow solid (215 mg, 96%). ¹H NMR (600 MHz, C₆D₆) δ 8.81 (dd, *J* = 8.2, 1.2 Hz, 2H), 8.04–7.95 (m, 6H), 7.43–7.32 (m, 3H), 7.23–7.18 (m, 3H), 7.15 (d, *J* = 1.4 Hz, 6H), 7.00 (dd, *J* = 7.5, 1.7 Hz, 2H), 6.96 (td, *J* = 7.3, 1.2 Hz, 2H), 6.73 (s, 2H). ³¹P-NMR (243 MHz, C₆D₆) δ 17.30 (s). ¹³C NMR (151 MHz, C₆D₆) δ 157.13 (s), 133.17 (d, *J* = 8.6 Hz), 132.73 (s), 131.11 (s), 130.82 (s), 130.62 (s), 130.22 (s), 128.43 (s), 128.00 (s), 127.82 (s), 127.60 (s), 121.94 (s), 121.72 (s). EA found: C 81.68%, H 5.63%, N 5.82%; calculated for C₃₂H₂₅N₂P: C 82.03%, H 5.38%, N 5.98%.

N-(Trimethylsilyl)-5*H*-dibenzo[*b,f*]azepin-5-amine (6)

A solution of LDA (0.625 g, 5.84 mmol) in THF (6 ml) was added dropwise to a solution of **2** (1.20 g, 5.74 mmol) in THF (10 ml). While stirring for 2 h, the reaction mixture turned red and an orange precipitate formed. A solution of TMSCl (0.750 g, 6.87 mmol, 0.88 ml, 1.2 eq.) in THF (4 ml) was added dropwise and the yellow solution was stirred for an additional 1 h. The solvent was removed, and the residue was extracted with benzene (10 ml) and centrifuged for 5 min at 5300 rpm. The decanted solution was cooled to –30 °C and subsequently the frozen benzene was sublimed in HV to afford a yellow powder (1.59 g, 99%). ¹H NMR: (270 MHz, C₆D₆) δ 7.07–7.00 (m, 2H, ArH), 6.88–6.85 (m, 2H, ArH), 6.76–6.74 (m, 4H, ArH), 6.49 (s, 2H, ArH), 3.75 (s, 1H, NH), 0.05 (s, 9H, Si(CH₃)₃). ¹³C NMR: (68 MHz, CDCl₃) δ 154.4 (s), 132.5 (s), 130.9 (s), 128.9 (s), 128.6 (s), 123.1 (s), 118.8 (s), –0.99 (s). EA found: C 72.65%, H 7.08%, N 9.50%; calculated for C₁₇H₂₀N₂Si: C 72.81%, H 7.19%, N 9.99%.

Tris-(lithium{*N*-(trimethylsilyl)-5*H*-dibenzo[*b,f*]azepin-5-amide}) (7)

PhLi (309 mg, 3.63 mmol) was suspended in toluene (13 ml) and added dropwise to a solution of **6** (1.01 g, 3.60 mmol) in toluene (3 ml). The red solution was stirred for 4 h at RT. Subsequently the solvent was removed to dryness to give a red foam and the crude was slurried in *n*-pentane (12 ml) for 6 h. The orange precipitate (933 mg, 87%) was filtered and dried in HV. ¹H NMR: (400 MHz, C₆D₆) δ 7.46 (m, 2H, ArH), 7.12 (m, 2H, ArH), 6.85 (m, 4H, ArH), 6.51 (m, 2H, ArH), 0.12 (br. s, 9H, Si(CH₃)₃). ¹³C NMR: (101 MHz, C₆D₆) δ 155.9 (s), 133.0 (s), 131.9 (s), 129.79 (s), 124.8 (s), 123.7 (s), 2.43. EA found: C

70.89%, H 6.73%, N 9.33%; calculated for C₁₇H₁₉N₂SiLi: C 71.30%, H 6.69%, N 9.78%.

N,N-Bis(trimethylsilyl)-5*H*-dibenzo[*b,f*]azepin-5-amine (8)

A solution of TMSCl (38.2 mg, 0.352 mmol) in THF (2 ml) was added dropwise to a solution of **7** (103 mg, 0.352 mmol) in THF (1.5 ml). The resulting red solution was stirred for 45 min at RT. Afterwards the solvent was removed to dryness and the crude was extracted with benzene (5 ml) and filtered over cotton and Celite in a pipette. The solution was cooled to –30 °C and the frozen benzene was sublimed in HV to afford the product as a yellow solid (125 mg, 100%). ¹H NMR: (400 MHz, C₆D₆) δ 7.09 (dd, 2H, ArH, ⁴*J*_{H,H} = 1 Hz, ³*J*_{H,H} = 8 Hz), 6.95–6.91 (m, 2H, ArH), 6.65 (dt, 2H, ArH, ⁴*J*_{H,H} = 1 Hz, ³*J*_{H,H} = 8 Hz), 6.58 (dd, 2H, ArH, ⁴*J*_{H,H} = 1 Hz, ³*J*_{H,H} = 8 Hz), 6.05 (s, 2H, ArH), 0.31 (s, 18H, Si(CH₃)₃). ¹³C NMR: (68 MHz, C₆D₆) δ 154.7, 133.8, 130.9, 130.8, 127.8, 122.6, 121.6, 2.25. EA found: C 67.97%, H 7.89%, N 7.51%; calculated for C₂₀H₂₈N₂Si₂: C 68.12%, H 8.00%, N 7.94%.

(2*Z*,4*E*)-4-((5*H*-Dibenzo[*b,f*]azepin-5-yl)imino)pent-2-en-2-ol (9)

2 (502 mg, 2.41 mmol) was dissolved in EtOH (6 ml) and acetyl acetate (0.250 ml, 2.41 mmol) was added. The yellow reaction solution was stirred for 10 d at RT and reaction progress was monitored by TLC. The solvent was removed and the remaining solid was dissolved in *n*-pentane. The solution was cooled to –30 °C in the fridge overnight. The formed crystals were filtered and dried to obtain the product as yellow crystals (576 mg, 80%). ¹H NMR: (400.13 MHz, CDCl₃) δ 13.1 (br. s, 1H, OH), 7.32–7.02 (m, 8H, ArH), 6.75 (s, 2H, ArH), 5.06 (s, 1H, =CH), 2.11 (s, 3H, CH₃), 1.95 (s, 3H, CH₃). ¹³C NMR (101 MHz, CDCl₃) δ 196.88 (s), 163.90 (s), 149.84 (s), 132.19 (s), 130.57 (s), 129.49 (s), 129.41 (s), 124.61 (s), 118.91 (s), 96.16 (s), 29.11 (s), 17.96 (s). EA found: C 78.78%, H 6.32%, N 9.54%; calculated for C₁₇H₁₈N₂O: C 78.59%, H 6.25%, N 9.65%.

(1*E*,2*E*)-*N*¹,*N*²-Bis(5*H*-dibenzo[*b,f*]azepin-5-yl)ethane-1,2-diimine (10)

2 (2.00 g, 9.60 mmol) was dissolved in EtOH (50 ml) and a glyoxal solution (0.55 ml, 4.80 mmol, 40 wt% in H₂O) was added *via* syringe. After 10 min a yellow precipitate formed, and the reaction mixture was stirred for additional 15 h. The solvent was removed and the solid was slurried in hexane (20 ml). The product was filtered, washed with cold hexane (3 × 5 ml) and dried in HV to obtain a yellow powder (1.83 g, 87%). ¹H NMR: (600.13 MHz, CDCl₃) δ 7.27–7.23 (m, 9H, ArH), 7.17–7.15 (m, 5H, ArH), 7.11–7.08 (m, 4H, ArH), 6.69 (s, 4H, ArH). ¹³C NMR: (150.9 MHz, CDCl₃) δ 144.6 (s), 135.7 (s), 134.3 (s), 130.9 (s), 130.0 (s), 129.6 (s), 127.0 (s), 126.8 (s). EA found: C 82.51%, H 5.09%, N 12.84%; calculated for C₃₀H₂₂N₄: C 82.17%, H 5.06%, N 12.78%.

(*E*)-2-((5*H*-Dibenzo[*b,f*]azepin-5-yl)imino)acenaphthylene-1(2*H*)-one (11)

Crystalline acenaphthylene-1,2-dione (1.03 g, 5.73 mmol) and **2** (1.22 g, 5.84 mmol) were placed in a flask with MeOH



(40 ml). The suspension turned orange, before an orange precipitate formed. Stirring was continued for 15 h, the solvent was removed, and the crude was washed with *n*-hexane (2 × 20 ml). After drying in HV the product was obtained as an orange powder (1.86 g, 87%) ¹H NMR (400 MHz, CDCl₃) δ (ppm) = 8.06 (d, *J* = 7.0 Hz, 1H), 7.99 (d, *J* = 8.1 Hz, 1H), 7.77–7.54 (m, 4H), 7.38–7.21 (m, 5H), 7.17 (td, *J* = 7.4, 1.1 Hz, 3H), 7.04 (s, 2H), 6.10 (d, *J* = 7.3 Hz, 1H) ¹³C NMR (101 MHz, CDCl₃) δ 189.96 (s), 149.00 (s), 141.22 (s), 140.09 (s), 131.86 (s), 131.59 (s), 131.52 (s), 131.38 (s), 130.41 (s), 129.80 (s), 129.38 (s), 127.93 (s), 127.89 (s), 127.64 (s), 126.70 (s), 126.02 (s), 123.72 (s), 123.07 (s), 121.71 (s). EA found: C 83.65%, H 4.17%, N 7.32%; calculated for C₂₆H₁₆N₂O C 83.85%, H 4.33%, N 7.52%.

N-(5*H*-Dibenzo[*b,f*]azepin-5-yl)propan-2-imine (12)

2 (1.04 g, 5.00 mmol) was dissolved in MeOH (20 ml) and acetone (0.400 ml, 5.50 mmol) was added *via* syringe. The reaction mixture was stirred for 3 d, during which time a yellow precipitate formed. Reaction progress was monitored by TLC and after complete conversion the solvent was removed and the crude washed with *n*-hexane (5 ml) and dried in HV to a bright yellow powder (1.11 g, 89%) ¹H NMR (600 MHz, CDCl₃) δ (ppm) = 7.75 (dd, *J* = 8.3, 1.2 Hz, 2H), 7.51 (ddd, *J* = 8.4, 7.2, 1.6 Hz, 2H), 7.36 (dd, *J* = 7.7, 1.6 Hz, 2H), 7.27–7.21 (m, 1H), 7.09 (s, 2H), 2.39 (s, 3H), 2.00 (s, 3H). ¹³C NMR (101 MHz, CDCl₃) δ 166.16 (s), 152.46 (s), 132.26 (s), 130.71 (s), 129.08 (s), 128.88 (s), 123.27 (s), 119.85 (s), 25.22 (s), 19.91 (s). EA found: C 82.40%, H 6.43%, N 11.35%; calculated for C₁₇H₁₆N₂: C 82.22%, H 6.49%, N 11.28%.

Lithium *N*-(5*H*-dibenzo[*b,f*]azepin-5-yl)propene-2-amide tris-tetrahydrofuranate (13)

12 (151 mg, 0.606 mmol) and LDA (68.2 mg, 0.636 mmol) were placed in a vial and THF (5 ml) was added. The deep red reaction mixture was stirred for 15 h, layered with *n*-hexane (6 ml), and cooled to –30 °C for crystallization. The mother liquor was decanted off and the remaining deep red crystals washed with *n*-hexane (4 ml) and dried in HV (153 mg, 60%). Despite measuring crystalline 13, NMR spectra always showed traces of 12 as impurity, which we attribute to partial hydrolysis of the product by adventitious water. ¹H NMR (400 MHz, THF-*d*₈) δ 6.93 (d, *J* = 8.6 Hz, 2H), 6.45 (t, *J* = 8.8 Hz, 2H), 6.6 (d, *J* = 7.2 Hz, 2H), 5.97 (d, *J* = 7.2 Hz, 2H), 5.20 (s, 2H), 3.64–3.51 (m, 4H, THF), 2.96 (s, 1H), 2.75 (s, 1H), 1.83–1.70 (m, 4H, THF), 1.52 (s, 3H). EA found: C 74.50%, H 7.75%, N 7.00%, calculated for C₁₇H₁₅N₂Li·2.35 C₄H₈O: C 74.84%, H 8.04%, N 6.61%.

N,1-Bis(5*H*-dibenzo[*b,f*]azepin-5-yl)-1,1-diphenyl-λ⁵-phosphine-imine (14)

To a suspension of [MesCu]₄ (101 mg, 0.423 mmol) in pyridine (5 ml), which was cooled to –30 °C, a cold solution (–30 °C) of 3 (168 mg, 0.422 mmol) in pyridine (2 ml) was added dropwise. The yellow solution turned red brown within 30 min. After stirring overnight at RT, the solvent was removed to dryness and the crude was slurried in *n*-pentane (8 ml) for

2.5 h. The precipitate was filtered, washed with *n*-pentane (5 ml) and dried in HV to afford the product as a light brown solid (172 mg, 61% with respect to 3). ¹H NMR: (600 MHz, C₆D₆) δ 8.64 (d, 2H, ArH, ³*J*_{H,H} = 12 Hz), 8.16–8.11 (m, 6H, ArH), 7.28–7.25 (m, 3H, ArH), 6.97–6.68 (m, 19H, ArH), ³¹P NMR: (243 MHz, C₆D₆) δ 16.9 (s). ¹³C NMR: (68 MHz, C₆D₆) δ 156.9 (d, ³*J*_{C,P} = 9 Hz), 144.0 (d, ²*J*_{C,P} = 5 Hz), 135.1 (s), 135.1 (s), 133.7 (s), 133.5 (s), 132.7 (s), 131.6 (s), 130.9 (s), 130.8 (s), 130.6 (t, ¹*J*_{C,P} = 1 Hz), 129.0 (s), 128.9 (s), 128.8 (s), 128.0 (s), 127.6 (s), 127.6 (s), 125.7 (s), 122.3 (s), 121.8 (s).

[Cu((2*Z*,4*E*)-4-((5*H*-Dibenzo[*b,f*]azepin-5-yl)imino)pentenoate)]₂ (15)

9 (111 mg, 0.381 mmol) and mesityl copper (91 mg, 0.38 mmol) were placed in a vial and toluene (5 ml) was added. The initial yellow reaction solution turned slowly from orange to deep brown. After stirring for 15 h the reaction solution was filtered over cotton and Celite to remove metallic Cu. The filtrate concentrated to half of the initial volume and layered with *n*-hexane (6 ml) at –30 °C. The complex was obtained as red brownish crystals (71 mg, 0.11 mmol, 58%) The paramagnetic complex is NMR silent. EA: found C 71.14%, H 5.37%, N 8.54%; calculated for C₃₈H₃₄N₄O₂Cu: C 71.06%, H 5.34%, N 8.72%.

[Cu(10)]₂PF₆ (16)

A solution of 10 (150 mg, 0.343 mmol) in DCM (4 ml) was added dropwise to a suspension of [Cu(CNCH₃)₄]PF₆ (128 mg, 0.343 mmol) in DCM (2 ml). An orange precipitate formed, and stirring was continued for 3 d. The solvent volume was reduced to a third and *n*-hexane (6 ml) was added to complete precipitation. The reaction mixture was cooled to –30 °C, filtered and washed with cold *n*-hexane (2 × 2 ml). After drying in HV the product was obtained as an orange powder (213 mg, 85%). ¹H NMR: (400 MHz, CD₂Cl₂) δ 7.48–7.32 (m, 25H, ArH), 6.97 (s, 8H, ArH), 6.97–6.88 (m, 7H, ArH), 6.32 (s, 4H, ArH). ¹³C NMR: (101 MHz, CD₂Cl₂) δ 134.6 (s), 130.7 (s), 130.4 (s), 129.9 (s), 128.4 (s), 128.1 (s), 127.8 (s). EA found: C 64.74%, H 3.89%, N 10.22%; calculated for C₆₀H₄₄CuN₈PF₆: C 64.80%, H 4.03%, N 10.01%.

[FeCl₂(10)] (17)

10 (300 mg, 0.684 mmol) and FeCl₂(THF)_{1.5} (161 mg, 0.684 mmol) were placed in a vial, suspended in 1,2-difluorobenzene (5 ml) and stirred overnight, while the suspension changed color from yellow to dark brown. For crystallization, the reaction vial was warmed with a heat gun until a clear solution was obtained and crystallization was completed by cooling down to –30 °C overnight. The liquid was decanted, and the crystals were washed with *n*-hexane (2 ml). The product was dried under vacuum and dark reddish crystals were obtained (374 mg, 97%). ¹H NMR (400 MHz, C₆D₆) δ 4.95 (br. s), 3.71 (br. s) EA found: C 64.02%; H, 3.89%; N, 9.76%; calculated for C₃₆H₂₈Cl₂FeN₄: C 63.74%; H 3.92%; N 9.91%.



[Cu(OTf)(11)]₂ (18)

A suspension of **11** (500 mg, 1.34 mmol) in toluene (10 ml) was added dropwise to [Cu(OTf)]₂·C₆H₆ (338 mg, 0.671 mmol) suspended in toluene (4 ml). Immediately an orange-brown precipitate formed, and the reaction mixture was stirred for 15 h. The solvent was removed, and the precipitate was washed with toluene (6 ml) and *n*-pentane (2 × 5 ml). After drying in HV, the complex was obtained as an orange powder (705 mg, 86%). ¹H NMR (400 MHz, CD₂Cl₂) δ 8.29 (d, *J* = 8.0 Hz, 2H), 7.85–7.72 (m, 4H), 7.58 (d, *J* = 8.0 Hz, 2H), 7.43–7.24 (m, 8H), 7.18 (dd, *J* = 11.1, 9.0 Hz, 4H), 7.07 (t, *J* = 7.8 Hz, 2H), 6.97 (d, *J* = 8.0 Hz, 2H), 6.80 (d, *J* = 7.8 Hz, 2H), 6.72 (t, *J* = 7.9 Hz, 2H), 6.25 (d, *J* = 9.8 Hz, 2H), 4.74 (d, *J* = 7.5 Hz, 2H). ¹⁹F NMR (400 MHz, CD₂Cl₂) δ –78.37 (s). ¹³C NMR (101 MHz, CD₂Cl₂) δ (ppm) = 194.25 (s), 146.25 (s), 141.28 (s), 139.86 (s), 138.46 (s), 133.29 (s), 133.24 (s), 131.38 (s), 130.24 (s), 130.07 (s), 129.86 (s), 128.91 (s), 128.87(s), 128.53 (s), 128.41 (s), 128.18 (s), 127.57 (s), 127.12 (s), 126.59 (s), 125.49 (s), 125.10 (s), 124.04 (s), 123.32 (s), 104.25 (s), 102.06 (s). EA found: C 54.00%, H 2.95%, N 4.57% S 5.39%; calculated for C₂₇H₁₆N₂O₄SF₃Cu·0.25 CH₂Cl₂: C 53.99%, H 2.74%, N 4.62%, S 5.29%.

[Cu(12)₂OTf (19)

A solution of **12** (945 mg, 3.81 mmol) in CH₂Cl₂ (15 ml) was added to a stirred slurry of [Cu(OTf)]₂·C₆H₆ (485 mg, 0.950 mmol) in CH₂Cl₂ (5 ml). After stirring the orange solution for 2 h at room temperature, the reaction solution was filtered over cotton and Celite. The dark yellow filtrate was concentrated to half of its volume and the product was precipitated by adding *n*-hexane (15 ml). The solid was filtered, washed with *n*-hexane (2 × 6 ml), and dried in HV to afford a yellow powder (1.23 g, 91%). ¹H NMR (400 MHz, CDCl₃) δ 7.55 (dd, *J* = 8.3, 1.4 Hz, 2H), 7.47 (m, 4H), 7.36 (td, *J* = 7.3, 1.4 Hz, 2H), 6.58 (s, 2H), 2.47 (s, 3H), 1.62 (s, 3H). ¹³C NMR (151 MHz, CDCl₃) δ 145.34 (s), 133.49 (s), 131.09 (s), 129.6 (s), 129.00 (s), 128.32 (s), 119.04 (s), 26.95 (s), 21.45 (s). EA found: C 59.14%, H 4.56%, N 7.93%, S 4.31%; calculated for C₃₅H₃₂N₄CuSO₃F₃: C 59.27%, H 4.55%, N 7.90%, S 4.52%. Diffraction quality single crystals were grown by layering a CH₂Cl₂ solution with *n*-pentane.

Single crystal X-ray structure determinations

Single crystal X-ray structure determinations were performed on a Bruker Kappa IμS Duo diffractometer using MoK_α radiation (λ = 0.71073 Å) and QUAZAR focusing Montel optics (for **7**, **13**, **14**, and **19**), a Bruker Smart diffractometer using MoK_α radiation (λ = 0.71073 Å, curved graphite monochromator) for **10**, an Agilent SuperNova dual radiation diffractometer with microfocus X-ray sources and mirror optics using MoK_α radiation (λ = 0.71073 Å for **11** and **18**) or CuK_α radiation (λ = 1.54184 Å for **15** and **17**). All intensity data sets were collected at a temperature of 100 K. The structures were solved with SHELXT⁶³ and were refined on F² with SHELXL 2018/3.⁶⁴ Further details are summarized in the ESI.†

Conflicts of interest

The authors have no conflicts of interest to declare.

Acknowledgements

We thank Mses Christina Wronna and Antigone Roth for carrying out the elemental analyses. Generous financial support for AG by Siemens Energy within the framework of the Energy Campus Erlangen-Nuremberg are gratefully acknowledged.

References

- 1 R. Lazny and A. Nodzewska, *N,N*-Dialkylhydrazones in Organic Synthesis. From Simple *N,N*-Dimethylhydrazones to Supported Chiral Auxiliaries, *Chem. Rev.*, 2010, **110**, 1386–1434.
- 2 (a) D. Enders and E. J. Corey, Herstellung Und Synthetische Verwendung von Metallierten Dimethylhydrazonen Regio-Und Stereoselektive Alkylierung von Carbonylverbindungen, *Chem. Ber.*, 1978, **111**, 1337–1361; (b) J. S. M. Lehn, S. Javed and D. M. Hoffman, Synthesis of Zirconium, Hafnium, and Tantalum Complexes with Sterically Demanding Hydrazide Ligands, *Inorg. Chem.*, 2007, **46**, 993–1000.
- 3 (a) R. H. Shapiro and M. J. Heath, Tosylhydrazones. V. Reaction of Tosylhydrazones with Alkylolithium Reagents. A New Olefin Synthesis, *J. Am. Chem. Soc.*, 1967, **89**, 5735. For a catalytic example, see: (b) K. Maruoka, M. Oishi and H. Yamamoto, The Catalytic Shapiro Reaction, *J. Am. Chem. Soc.*, 1996, **118**, 2289–2290.
- 4 (a) A. Bermejo, A. Ros, R. Fernández and J. M. Lassaletta, C₂-Symmetric Bis-Hydrazones as Ligands in the Asymmetric Suzuki-Miyaura Cross-Coupling, *J. Am. Chem. Soc.*, 2008, **130**, 15798–15799; (b) B. Sedai, M. J. Heeg and C. H. Winter, Volatility Enhancement in Calcium, Strontium, and Barium Complexes Containing β-Diketiminato Ligands with Dimethylamino Groups on the Ligand Core Nitrogen Atoms, *Organometallics*, 2009, **28**, 1032–1038 and ref. 2b (c) D. F.-J. Piesik, R. Stadler, S. Range and S. Harder, Binuclear Magnesium, Calcium, and Zinc Complexes Based on Nitrogen–Nitrogen-Coupled Salicylaldiminate and β-Diketiminato Ligands, *Eur. J. Inorg. Chem.*, 2009, 3569–3576; (d) J. Intemann, J. Spielmann, P. Sirsch and S. Harder, Well-Defined Molecular Magnesium Hydride Clusters: Relationship between Size and Hydrogen-Elimination Temperature, *Chem. – Eur. J.*, 2013, **19**, 8478–8489; (e) J. Intemann, P. Sirsch and S. Harder, Comparison of Hydrogen Elimination from Molecular Zinc and Magnesium Hydride Clusters, *Chem. – Eur. J.*, 2014, **20**, 11204–11213. For the use of monodentate hydrazide ligands, see for example: (f) J. S. M. Lehn, S. Javed and D. M. Hoffman, Synthesis of Zirconium, Hafnium, and Tantalum Complexes with Sterically Demanding Hydrazide Ligands, *Inorg. Chem.*, 2007, **46**,



- 993–1000. For applications in catalysis, see for example: (g) T. Mino, Y. Shirae, Y. Sasai, M. Sakamoto and T. Fujita, Phosphine-Free Palladium Catalyzed Mizoroki-Heck Reaction Using Hydrazone as a Ligand, *J. Org. Chem.*, 2006, **71**, 6834–6839; (h) T. Mino, M. Shibuya, S. Suzuki, K. Hirai, M. Sakamoto and T. Fujita, Palladium-Catalyzed Mizoroki-Heck Type Reaction with Aryl Trialkoxysilanes Using Hydrazone Ligands, *Tetrahedron*, 2012, **68**, 429–432.
- 5 For historical examples of α -dihydrazone ligands, see: (a) H. D. Hausen and K. Krogmann, Die Kristallstruktur von Dicarboxyl-diacyl-bis(dimethylhydrazon)-Ni(0), *Z. Anorg. Allg. Chem.*, 1972, **389**, 247–253; (b) P. Ammendola, M. R. Ciajolo, A. Panunzi and A. Tuzi, Trigonal bipyramidal platinum complexes as models for Ziegler-Natta catalytic sites, *J. Organomet. Chem.*, 1983, **254**, 389–397; (c) J. Ehlers and H. Tom Dieck, Modellkomplexe Mit Hydrazonchelaten von (S)- und (R)-1-Amino-2-Methoxymethylpyrrolidin ("SAMP" and "RAMP") Und Dimethylhydrazine - Struktur Des (Pyridinaldehyd-RAMP-Hydrazon-Tetracarbonyl-Molybdäns, *Z. Anorg. Allg. Chem.*, 1988, **560**, 80–92. For β -dihydrazone ligands, see: (d) G. Bocelli, A. Cantoni and G. Tosi, Structure of Butanedione Bis (Methylphenylhydrazone), *Acta Crystallogr., Sect. C: Cryst. Struct. Commun.*, 1992, **48**, 1041–1043.
- 6 (a) C. Defieber, M. A. Ariger, P. Moriel and E. M. Carreira, *Angew. Chem., Int. Ed.*, 2007, **46**, 3139; (b) A. Briceño and R. Dorta, *Acta Crystallogr., Sect. E: Struct. Rep. Online*, 2007, **63**, m1718–m1719; (c) R. Mariz, A. Briceno, R. Dorta and R. Dorta, *Organometallics*, 2008, **27**, 6605; (d) E. Drinkel, A. Briceno, R. Dorta and R. Dorta, *Organometallics*, 2010, **29**, 2503; (e) T. J. Hoffman and E. M. Carreira, *Angew. Chem., Int. Ed.*, 2011, **50**, 10670; (f) M. Roggen and E. M. Carreira, *Angew. Chem., Int. Ed.*, 2011, **50**, 5568; (g) M. Lafrance, M. Roggen and E. M. Carreira, *Angew. Chem., Int. Ed.*, 2012, **51**, 3470; (h) A. Herrera, A. Grasruck, F. W. Heinemann, A. Scheurer, A. Chelouan, S. Frieß, F. Seidel and R. Dorta, *Organometallics*, 2017, **36**, 714; (i) A. Chelouan, S. Bao, S. Frieß, A. Herrera, F. W. Heinemann, A. Escalona, A. Grasruck and R. Dorta, *Organometallics*, 2018, **37**, 3983; (j) L. Leinauer, G. Parla, J. Messelberger, A. Herrera, F. W. Heinemann, J. Langer, I. Chuchelkin, A. Grasruck, S. Frieß, A. Chelouan, K. Gavrillov and R. Dorta, Evolution of a 'privileged' P-alkene ligand: added planar chirality beats BINOL axial chirality in catalytic asymmetric C–C bond formation, *Chem. Commun.*, 2023, **59**, 13879–13882.
- 7 (a) A. Grasruck, G. Parla, F. W. Heinemann, J. Langer, A. Herrera, S. Frieß, G. Schmid and R. Dorta, *New J. Chem.*, 2023, **47**, 2307; (b) A. Grasruck, G. Parla, L. Lou, F. W. Heinemann, J. Langer, C. Christian Neiß, A. Herrera, S. Frieß, A. Görling, G. Schmid and R. Dorta, Trapping of soluble, KCl-stabilized Cu(I) hydrides with CO₂ gives crystalline formates, *Chem. Commun.*, 2023, **59**, 13879–13882; (c) A. Grasruck, G. Parla, F. W. Heinemann, J. Langer, A. Herrera, S. Frieß, G. Schmid and R. Dorta, Developing bulky P-alkene ligands: stabilization of copper complexes with 14 valence electrons, *New J. Chem.*, 2023, **47**, 2307–2323.
- 8 (a) F. Breher, C. Böhrer, G. Frison, J. Harmer, L. Liesum, A. Schweiger and H. Grützmacher, TROPDAD: A New Ligand for the Synthesis of Water-Stable Paramagnetic [16+1]-Electron Rhodium and Iridium Complexes, *Chem. – Eur. J.*, 2003, **9**, 3859–3866; (b) T. Büttner, F. Breher and H. Grützmacher, Amine olefin rhodium(I) complexes: pK_a and NH bond strength, *Chem. Commun.*, 2004, 2820–2821.
- 9 (a) D. Bogdal, Carbazolyl Nitrenium Cations: Generation and Reaction, *Heterocycles*, 2000, **53**, 1–29; (b) A. H. Winter, H. H. Gibson and D. E. Falvey, Carbazolyl Nitrenium Ion: Electron Configuration and Antiaromaticity Assessed by Laser Flash Photolysis, Trapping Rate Constants, Product Analysis, and Computational Studies, *J. Org. Chem.*, 2007, **72**, 8186–8195.
- 10 I. A. Tonks, A. C. Durrell, H. B. Gray and J. E. Bercaw, Groups 5 and 6 Terminal Hydrazido(2-) Complexes: N β Substituent Effects on Ligand-to-Metal Charge-Transfer Energies and Oxidation States, *J. Am. Chem. Soc.*, 2012, **134**, 7301–7304.
- 11 R. P. Nielsen and H. H. Sisler, Hydrazinophosphorus Compounds. I. Preparation, of Some Substituted Hydrazinophosphines, Hydrazinophosphine Oxides, and Hydrazinophosphine Sulfides, *Inorg. Chem.*, 1963, **2**, 753–760.
- 12 PBr₂Ph₃ was not used *in situ* as usual for such reactions and was isolated in 97% yield (see experimental section). See also: J. P. Schaefer, J. G. Higgins and P. K. Shenoy, Cinnamyl Bromide, *Org. Synth.*, 1968, **48**, 51.
- 13 T. Bauer, S. Schulz, M. Nieger and U. Kessler, Bis (Alkylamino)Phosphanes: Deprotonation Reactions and Reactivity of t-BuP(NH-t-Bu)₂ toward Group 13 Metalloorganics, *Organometallics*, 2003, **22**, 3134–3142.
- 14 (a) H. Zimmer and G. Singh, Reaktion von Triphenylphosphinimininen Mit Nitrosylchlorid, *Angew. Chem., Int. Ed. Engl.*, 1963, **75**(12), 574–574; (b) H. Zimmer, M. Jayawant and P. Gutsch, Synthesis of Secondary Amines via Triphenylphosphinimines, *J. Org. Chem.*, 1970, **35**, 2826–2828.
- 15 (a) H. Zimmer and G. Singh, Synthesis and Some Reactions of Triphenylphosphinamino- and (β -N-Disubstituted Amino)Imines, *J. Org. Chem.*, 1964, **29**(6), 1579–1581; (b) M. T. Reetz and J. Rheinheimer, Synthesis and Properties of Cyclopropanone Hydrazones, *J. Org. Chem.*, 1986, **51**, 5465–5467.
- 16 (a) O. J. Scherer and W. Gläsel, 1-Tert.-Butyl-3-Trimethylsilyl-4,4-Dimethyl-2-Phospha-1-Tetrazen, *Angew. Chem., Int. Ed. Engl.*, 1975, **87**, 667–668; (b) M. F. Lappert, M. J. Slade, A. Singh, J. L. Atwood, R. D. Rogers and R. Shakir, Structure and Reactivity of Sterically Hindered Lithium Amides and Their Diethyl Etherates: Crystal and Molecular Structures of [Li(N(SiMe₃)₂)(OEt₂)]₂ and Li(NCMe₂CH₂CH₂CH₂CMe₂)₄, *J. Am. Chem. Soc.*, 1983, **105**, 302–304.



- 17 (a) B. Gemünd, H. Nöth, H. Sachdev and M. Schmidt, Structural Chemistry of Alkali Metal Phenylhydrazides, *Chem. Ber.*, 1996, **129**, 1335–1344; (b) M. G. Voronkov, B. A. Gostevskij, B. A. Shajnyan, V. I. Rakhlin, R. G. Mirskov and O. S. Makarova, Reaction of Organosilicon Derivatives of 1,1-Dimethylhydrazine with Methyl iodide, *Dokl. Chem.*, 2005, **400**, 17–20; (c) C. Keck, C. Maichle-Mossmer and H. F. Bettinger, Photo Electron Transfer Induced Desilylation of: N,N-Bis(Trimethylsilyl) Aminodibenzoborole to Aminodibenzoborole, *Chem. Commun.*, 2019, **55**, 7470–7473.
- 18 J. Ru Hwu and N. Wang, Counterattack Reagents: Hexamethyldisilane and 1,2-Dimethyl-1,1,2,2-Tetraphenyldisilane in the Synthesis of Polysilylated Hydrazines, *Tetrahedron*, 1988, **44**, 4181–4196.
- 19 D. R. Armstrong, K. W. Henderson, A. R. Kennedy, W. J. Kerr, F. S. Mair, J. H. Moir, P. H. Moran and R. Snaith, Structural Studies of the Chiral Lithium Amides $[\{\text{PhC}(\text{H})\text{Me}\}_2\text{NLi}]$ and $[\text{PhCH}_2\{\text{PhC}(\text{H})\text{Me}\}\text{NLi}\cdot\text{THF}]$ Derived from α -Methylbenzylamine, *J. Chem. Soc., Dalton Trans.*, 1999, 4063–4068.
- 20 For a good discussion and definitions of agostic vs. anagostic interactions, see: (a) M. Brookhart, M. L. H. Green and G. Parkin, *Proc. Natl. Acad. Sci. U. S. A.*, 2007, **104**, 6908; (b) D. Braga, F. Grepioni, K. Biradha and G. R. Desiraju, Agostic Interactions in Organometallic Compounds. A Cambridge Structural Database Study, *J. Chem. Soc., Dalton Trans.*, 1996, 3925–3930.
- 21 A. Herrera, A. Grasruck, F. W. Heinemann, A. Scheurer, A. Chelouan, S. Frieß, F. Seidel and R. Dorta, Developing P-Stereogenic, Planar-Chiral P-Alkene Ligands: Monodentate, Bidentate, and Double Agostic Coordination Modes on Ru(II), *Organometallics*, 2017, **36**, 714–720.
- 22 (a) M. Stender, R. J. Wright, B. E. Eichler, J. Prust, M. M. Olmstead, H. W. Roesky and P. P. Power, The Synthesis and Structure of Lithium Derivatives of the Sterically Encumbered β -Diketiminato Ligand $[\{(2,6\text{-Pri}_2\text{H}_3\text{C}_6\text{N}(\text{CH}_3)\text{C}_2\text{CH})\}_2\text{Li}^+\text{Li}^-\text{THF}]$, and a Modified Synthesis of the Aminoimine Precursor, *J. Chem. Soc., Dalton Trans.*, 2001, (23), 3465–3469; (b) J. Feldman, S. J. McLain, A. Parthasarathy, W. J. Marshall, J. C. Calabrese and S. D. Arthur, Electrophilic Metal Precursors and a β -Diimine Ligand for Nickel(II)- and Palladium(II)-Catalyzed Ethylene Polymerization, *Organometallics*, 1997, **16**, 1514–1516.
- 23 (a) N. Kuhn and H. Lanfermann, Synthese von N-Tert-Butyl-4-(Tert-Butylimino)-2-Penten-2-Amin, *Liebigs Ann. Chem.*, 1987, **6**, 727–728; (b) D. F. J. Piesik, R. Stadler, S. Range and S. Harder, Binuclear Magnesium, Calcium, and Zinc Complexes Based on Nitrogen-Nitrogen-Coupled Salicylaldimine and β -Diketiminato Ligands, *Eur. J. Inorg. Chem.*, 2009, (24), 3569–3576.
- 24 J. Vicente, M. T. Chicote, A. J. Martínez-Martínez, D. Bautista and P. G. Jones, Synthesis of a Family of 3-Alkyl- or 3-Aryl-Substituted 1,2-Dihydroquinazolinium Salts and Their Isomerization to 4-Iminium-1,2,3,4-Tetrahydroquinolines, *Org. Biomol. Chem.*, 2011, **9**(7), 2279–2285.
- 25 Assignment of the *cis/trans* conformation is prevented by overlapping signals of the aromatic and imine protons.
- 26 (a) N. Muresan, C. C. Lu, M. Ghosh, J. C. Peters, M. Abe, L. M. Henling, T. Weyhermüller, E. Bill and K. Wieghardt, Bis(α -Diimine)Iron Complexes: Electronic Structure Determination by Spectroscopy and Broken Symmetry Density Functional Theoretical Calculations, *Inorg. Chem.*, 2008, **47**, 4579–4590; (b) V. C. Gibson, R. K. O'Reilly, W. Reed, D. F. Wass, A. J. P. White and D. J. Williams, Four-Coordinate Iron Complexes Bearing α -Diimine Ligands: Efficient Catalysts for Atom Transfer Radical Polymerisation (ATRP), *Chem. Commun.*, 2002, **8**, 1850–1851.
- 27 Acenaphthoquinone usually reacts with 2 equiv. of amine to afford very stable BIAN (bis(aryl)acenaphthene quinone-diimine) α -diimines. (a) M. Gasperini, F. Ragaini and S. Cenini, Synthesis of Ar-BIAN Ligands (Ar-BIAN = Bis(Aryl)Acenaphthenequinone-diimine) Having Strong Electron-Withdrawing Substituents on the Aryl Rings and Their Relative Coordination Strength toward Palladium(0) and-(II) Complexes, *Organometallics*, 2002, **21**, 2950–2957. For examples of catalytic applications of BIAN ligands, see: (b) M. Laren and C. J. van Elsevier, Selective Homogeneous Palladium (0)-Catalyzed Hydrogenation of Alkynes to (Z)-Alkenes, *Angew. Chem., Int. Ed.*, 1999, **38**, 3715–3717; (c) F. Ragaini, S. Cenini, S. Tollari, G. Tummolillo and R. Beltrami, Allylic Amination of Unactivated Olefins by Nitroarenes, Catalyzed by Ruthenium Complexes. A Reaction Involving an Intermolecular C-H Functionalization, *Organometallics*, 1999, **18**, 928–942; (d) F. S. Wekesa, R. Arias-Ugarte, L. Kong, Z. Sumner, G. P. McGovern and M. Findlater, Iron-Catalyzed Hydrosilylation of Aldehydes and Ketones under Solvent-Free Conditions, *Organometallics*, 2015, **34**, 5051–5056.
- 28 The C2–O1, C1–N1, and C1–C2 distances are in the range of reported values of comparable structures. Cf. e.g.: J. Kovach, M. Peralta, W. W. Brennessel and W. D. Jones, Synthesis and X-Ray Crystallographic Characterization of Substituted Aryl Imines, *J. Mol. Struct.*, 2011, **992**, 33–38. ref. [5b].
- 29 (a) R. Von Bülow, H. Gornitzka, T. Kottke and D. Stalke, Dimers of Thf-Solvated Lithium Anilide and Lithium Pentafluoroanilide: Basic Building Blocks of Lithium Amide Ladder Structures, *Chem. Commun.*, 1996, **982**(14), 1639–1640; (b) D. B. Grotjahn, P. M. Sheridan, I. Al Jihad and L. M. Ziurys, First Synthesis and Structural Determination of a Monomeric, Unsolvated Lithium Amide, *J. Am. Chem. Soc.*, 2001, **123**, 5489–5494.
- 30 F. H. Allen, O. Kennard, D. G. Watson, L. Brammer, A. G. Orpen and R. Taylor, Tables of Bond Lengths Determined by X-Ray and Neutron Diffraction. Part 1. Bond Lengths in Organic Compounds, *J. Chem. Soc., Perkin Trans.*, 1987, **12**, 1–19.



- 31 M. P. Sadashiva, B. H. Doreswamy, K. S. Basappa, K. S. Rangappa, M. A. Sridhar and J. Shashidhara Prasad, Synthesis and Crystal Structure of 5-Allyl-5H-dibenzo[*b,f*]azepine, *J. Chem. Crystallogr.*, 2005, **35**(3), 171–175.
- 32 A. Herrera, A. Grasruck, F. W. Heinemann, A. Scheurer, A. Chelouan, S. Frieß, F. Seidel and R. Dorta, Developing P-Stereogenic, Planar-Chiral P-Alkene Ligands: Monodentate, Bidentate, and Double Agostic Coordination Modes on Ru(II), *Organometallics*, 2017, **36**, 714–720.
- 33 For a recent example of highly reactive, P-alkene-stabilized Cu(I) hydrides for CO₂ reduction, see ref. 7.
- 34 (a) S. D. J. Brown, W. Henderson, K. J. Kilpin and B. K. Nicholson, Orthomercurated and Cycloaurated Derivatives of the Iminophosphorane Ph₃P=NPh, *Inorg. Chim. Acta*, 2007, **360**, 1310–1315; (b) K. T. K. Chan, L. P. Spencer, J. D. Masuda, J. S. J. McCahill, P. Wei and D. W. Stephan, Anionic Phosphinimine-Chelate Complexes of Rhodium and Iridium: Steric and Electronic Influences on Oxidative Addition of CH₂Cl₂, *Organometallics*, 2004, **23**, 381–390.
- 35 C. Hettstedt, P. Köstler, E. Ceylan and K. Karaghiosoff, Synthesis of the First Representatives of Amino Bis(Picolyl) and Amino Bis(Quinaldinyl) Phosphines, *Tetrahedron*, 2016, **72**, 3162–3170.
- 36 (a) M. Stollenz and F. Meyer, Mesitylcopper - A Powerful Tool in Synthetic Chemistry, *Organometallics*, 2012, **31**(22), 7708–7727; (b) T. Tsuda, T. Hashimoto and T. Saegusa, Cuprous Tert-Butoxide., a New and Useful Metalation Reagent, *J. Am. Chem. Soc.*, 1972, **94**(2), 658–659.
- 37 (a) A. R. Cowley, J. R. Dilworth, A. K. Nairn and A. J. Robbie, Preparation and Characterization of Diarylphosphazene and Diarylphosphinohydrazide Complexes of Titanium, Tungsten and Ruthenium and Phosphorylketimido Complexes of Rhenium, *Dalton Trans.*, 2005, (4), 680–693; (b) S. K. Vasisht, G. Singh and P. K. Verma, Reactions of Bis (Trimethylsilyl) Amine and -Amide with MoOCl₄, *Monatsh. Chem.*, 1986, **117**, 177–183.
- 38 (a) A. J. Peel, J. Slaughter and A. E. H. Wheatley, New Options in Directed Cupration: Studies in Heteroleptic Bis (Amido)Cuprate Formation Dedicated to the Memory of Jack Lewis, *J. Organomet. Chem.*, 2016, **812**, 259–267; (b) J. Haywood, J. V. Morey, E. H. A. Wheatley, C. Y. Liu, S. Yasuike, J. Kurita, M. Uchiyama and P. R. Raithby, Gilman-Type versus Lipshutz-Type Reagents: Competition in Lithiocuprate Chemistry, *Organometallics*, 2009, **28**, 38–41; (c) P. J. Harford, A. J. Peel, F. Chevallier, R. Takita, F. Mongin, M. Uchiyama and A. E. H. Wheatley, New Avenues in the Directed Deprotometallation of Aromatics: Recent Advances in Directed Cupration, *Dalton Trans.*, 2014, **43**, 14181–14203.
- 39 Disproportionation reactions are often observed with related β-diketonate ligands systems and Cu(I) bases: (a) A. T. Larson, A. S. Crossman, S. M. Krajewski and M. P. Marshak, Copper(II) as a Platform for Probing the Steric Demand of Bulky β-Diketonates, *Inorg. Chem.*, 2020, **59**, 423–432; (b) B. Cheng, H. Yi, C. He, C. Liu and A. Lei, Revealing the Ligand Effect on Copper(I) Disproportionation via Operando IR Spectra, *Organometallics*, 2015, **34**, 206–211.
- 40 For examples of monomeric naccac-copper complexes, see: (a) D. S. Laitar, C. J. N. Mathison, W. M. Davis and J. P. Sadighi, Copper(I) Complexes of a Heavily Fluorinated β-Diketiminato Ligand: Synthesis, Electronic Properties, and Intramolecular Aerobic Hydroxylation, *Inorg. Chem.*, 2003, **42**, 7354–7356; (b) A. K. Gupta and W. B. Tolman, Cu(I)/O₂ Chemistry Using a β-Diketiminato Supporting Ligand Derived from N,N-Dimethylhydrazine: A [Cu₃O₂] 3+ Complex with Novel Reactivity, *Inorg. Chem.*, 2012, **51**, 1881–1888; (c) J. Takaichi, K. Ohkubo, H. Sugimoto, M. Nakano, D. Usa, H. Maekawa, N. Fujieda, N. Nishiwaki, S. Seki, S. Fukuzumi, *et al.*, Copper Complexes of the Non-Innocent β-Diketiminato Ligand Containing Phenol Groups, *Dalton Trans.*, 2013, **42**, 2438–2444.
- 41 D. Gao, M. Parvez and T. G. Back, Synthesis of Indoles by Conjugate Addition and Ligand-Free Copper-Catalyzed Intramolecular Arylation of Activated Acetylenes with o-Haloanilines, *Chem. – Eur. J.*, 2010, **16**(48), 14281–14284.
- 42 (a) P. A. Stabnikov, I. A. Baidina, S. V. Sysoev, N. S. Vanina, N. B. Morozova and I. K. Igumenov, Saturated Vapor Pressure and Crystal Structure of Bis-(2-Imino-4-Pentanonato)Copper(II), *J. Struct. Chem.*, 2003, **44**(6), 1054–1061; (b) G. R. Clark, D. Hall and T. N. Waters, The Colour Isomerism and Structure of Some Copper Co-Ordination Compounds. Part XV. The Crystal Structure of N, N-Ethylene-Bis(Acetylacetonato)Copper(II) Hemihydrate, *J. Chem. Soc.*, 1968, **1959**, 203–206.
- 43 For similar cationic Cu(I)-α-diimine complexes, see for example: B. Zelenay, R. Frutos-Pedreño, J. Markalain-Barta, E. Vega-Isa, A. J. P. White and S. Díez-González, Homo- and Heteroleptic Copper(I) Complexes with Diazabutadiene Ligands: Synthesis, Solution- and Solid-State Structural Studies, *Eur. J. Inorg. Chem.*, 2016, 4649–4658.
- 44 For selected examples of iron-α-diimine complexes, see ref. 22 and: (a) S. C. Bart, E. J. Hawrelak, A. K. Schmisser, E. Lobkovsky and P. J. Chirik, Synthesis, Reactivity, and Solid State Structures of Four-Coordinate Iron(II) and Manganese(II) Alkyl Complexes, *Organometallics*, 2004, **23**(2), 237–246; (b) H. Lee, M. G. Campbell, R. Hernández Sánchez, J. Börgel, J. Raynaud, S. E. Parker and T. Ritter, Mechanistic Insight into High-Spin Iron(I)-Catalyzed Butadiene Dimerization, *Organometallics*, 2016, **35**, 2923–2929.
- 45 For a discussion regarding the ring flip of the dibenzo[*b,f*]azepine rings, see: J. C. Calderón, A. Herrera, F. W. Heinemann, J. Langer, A. Linden, A. Chelouan, A. Grasruck, R. Añez, T. Clark and R. Dorta, Stereochemical Stability of Planar-Chiral Benzazepine Tricyclics: Inversion Energies of P- and S-Alkene Ligands, *J. Org. Chem.*, 2023, **88**, 16144–16154.
- 46 For a ligand that reacts with Cu(I) halide, see ref. 5b.
- 47 E. S. Chernyshova, R. Goddard and K.-R. Pörschke, *cis,cis*, *cis*-1,5,9-Cyclododecatriene-Metal Complexes, *Organometallics*, 2007, **26**, 4872–4880.



- 48 For a stilbenyl-Cu(I) triflate, see: (a) B. J. Barrett and V. Iluc, Coordination of a Hemilabile Pincer Ligand with an Olefinic Backbone to Mid-to-Late Transition Metals, *Inorg. Chem.*, 2014, **53**, 7248–7259. For Cu(I)-ethylene structures, see for example: (b) P. Ebrahimpour, M. F. Haddow and D. F. Wass, New Cu(I)-Ethylene Complexes Based on Tridentate Imine Ligands: Synthesis and Structure, *Inorg. Chem.*, 2013, **52**, 3765–3771; (c) H. Masuda, N. Yamamoto, T. Taga and S. Kitagawa, Structural Studies of Copper(I) [Cu(2,2'-Bipyridine)(Ethylene)]ClO₄, and [Cu(1,10-Phenanthroline)(Ethylene)]ClO₄, *J. Organomet. Chem.*, 1987, **322**, 121–129.
- 49 C. R. Martinez and B. L. Iverson, Rethinking the Term “Pi-Stacking”, *Chem. Sci.*, 2012, **3**(7), 2191–2201.
- 50 This is slightly longer than in comparable [Cu(L)CO(OTf)] complexes: (a) G. Doyle, K. A. Eriksen and D. V. Engen, Preparation of Copper(I) Carbonyl Complexes Derived from Sulfonic Acids. Crystal Structure of Cu(CO)C₂H₅SO₃, *Inorg. Chem.*, 1983, (22), 2892–2895; (b) P. J. J. A. Timmermans, A. Mackor, A. L. Spek and B. Kojic-Prodic, The Crystal and Molecular Structure of Copper(I) Trifluoromethanesulphonate Cyclohexene Complex, *J. Organomet. Chem.*, 1984, **276**, 287–295. But shorter compared to poly-alkene or -alkyne supported structures: J. D. Ferrara, C. Tessler-Youngs and W. J. Youngs, Synthesis and Characterization of a Copper(I) Triflate Complex of 1,2 : 5,6 : 9,10-Trisbenzo-Cyclododeca-1,5,9-Triene-3,7,11-Triyne, *Organometallics*, 1987, **6**, 676–678.
- 51 There is only a limited number of published Cu(I) BIAN complexes. (a) L. Li, P. S. Lopes, V. Rosa, C. A. Figueira, M. Amélia, N. D. A. Lemos, M. T. Duarte, T. Avilés and P. T. Gomes, Synthesis and Structural Characterisation of (Aryl-BIAN)Copper(I) Complexes and Their Application as Catalysts for the Cycloaddition of Azides and Alkynes, *Dalton Trans.*, 2012, **41**, 5144–5154; (b) V. Rosa, C. I. M. Santos, R. Welter, G. Aullón, C. Lodeiro and T. Avilés, Comparison of the Structure and Stability of New α -Diimine Complexes of Copper(I) and Silver(I): Density Functional Theory versus Experimental, *Inorg. Chem.*, 2010, **49**, 8699–8708.
- 52 Complexation of mesityl copper with ligand 7 only afforded untractable reaction products.
- 53 (a) S. Fraysse, V. von Zelewsky and H. Stoeckli-Evans, A Stable Chiral Diolefin Complex of CuI with Predetermined Configuration at the Metal Centre, *New J. Chem.*, 2001, **25**, 1374–1375; (b) J. Zhang, R. G. Xiong, J. L. Zuo, C. M. Che and X. Z. You, Highly Stable Copper(I)-Olefin Coordination Polymers Capable of Co-Existing with Water and Acid, *J. Chem. Soc., Dalton Trans.*, 2000, (17), 2898–2900.
- 54 (a) B. Gustafsson, M. Håkansson and S. Jagner, Copper(II) Is Harder than Copper(I): A Novel Mixed-Valence Example from Alkoxide Chemistry, *New J. Chem.*, 2003, **27**, 459–461; (b) G. Santiso-Quiñones, A. Reisinger, J. Slattery and I. Krossing, Homoleptic Cu-Phosphorus and Cu-Ethene Complexes, *Chem. Commun.*, 2007, **47**, 5046–5048.
- 55 (a) A. Linden, L. Llovera, J. Herrera, R. Dorta, G. Agrifoglio and R. Dorta, *Organometallics*, 2012, **31**, 6162; (b) R. Mariz, A. Briceño, R. Dorta and R. Dorta, *Organometallics*, 2008, **27**, 6605–6613.
- 56 J. J. Allen and A. R. Barron, Olefin, Coordination in Copper (I) Complexes of Bis(2-Pyridyl)Amine, *Dalton Trans.*, 2009, 878–890.
- 57 C. Floriani, E. M. Meyer, S. Gambarotta, A. Chiesi-Villa and C. Guastini, Polynuclear Aryl Derivatives of Group 11 Metals: Synthesis, Solid State-Solution Structural Relationship, and Reactivity with Phosphines, *Organometallics*, 1989, **8**, 1067–1079.
- 58 J. Kubas, Tetrakis(Acetonitrile)Copper(I) Hexafluorophosphate (1-), in *Inorganic synthesis*, ed. R. J. Angelici, 1990, vol. 28, pp. 68–70.
- 59 T. Cohen, R. J. Ruffner, D. W. Shull, E. R. Fogel and J. Falck, Vinyl Sulfides From Thioacetals With Copper(I) Trifluoromethanesulfonate: (Z)-2-Methoxy-1-Phenylthio-1,3-Butadiene, *Org. Synth.*, 1979, **59**, 202.
- 60 G. R. Fulmer, A. J. M. Miller, N. H. Sherden, H. E. Gottlieb, A. Nudelman, B. M. Stoltz, J. E. Bercaw and K. I. Goldberg, NMR Chemical Shifts of Trace Impurities: Common Laboratory Solvents, Organics, and Gases in Deuterated Solvents Relevant to the Organometallic Chemist, *Organometallics*, 2010, **29**(9), 2176–2179.
- 61 J. P. Schaefer, J. G. Higgins and P. K. Shenoy, Cinnamyl Bromide, *Org. Synth.*, 1968, **48**, 51.
- 62 H. Zimmer and G. Singh, Synthesis and Some Reactions of Triphenylphosphinamino- and (β -N-Disubstituted Amino) Imines, *J. Org. Chem.*, 1964, **29**(6), 1579–1581.
- 63 G. M. Sheldrick, A short history of SHELX, *Acta Crystallogr., Sect. A: Found. Crystallogr.*, 2008, **64**, 112–122.
- 64 G. M. Sheldrick, Crystal structure refinement with SHELXL, *Acta Crystallogr., Sect. C: Struct. Chem.*, 2015, **71**, 3–8.

